

USING SPIDER THEORY TO EXPLORE PARAMETER
SPACES

A Dissertation

Presented to the Faculty of the Graduate School
of Cornell University

in Partial Fulfillment of the Requirements for the Degree of
Doctor of Philosophy

by

David Anthony Brown

August 2001

© David Anthony Brown 2001

ALL RIGHTS RESERVED

USING SPIDER THEORY TO EXPLORE PARAMETER SPACES

David Anthony Brown, Ph.D.

Cornell University 2001

For a fixed integer $d \geq 2$, consider the family of polynomials $P_{d,\lambda}(z) = \lambda \left(1 + \frac{z}{d}\right)^d$, where λ is a complex parameter. In this work, we study the location of parameters λ for which $P_{d,\lambda}$ has an attracting cycle of a given length, multiplier, and combinatorial type.

Two main tools are used in determining an algorithm for finding these parameters: the well-established theories of external rays in the dynamical and parameter planes and Teichmüller theory. External rays are used to specify hyperbolic components in parameter space of the polynomials and study the combinatorics of the attracting cycle. A properly normalized space of univalent mappings is then employed to determine a linearizing neighborhood of the attracting cycle.

Since the image of a univalent mapping completely determines the mapping, we visualize these maps concretely on the Riemann sphere; with discs for feet and curves as legs connected at infinity, these maps conjure a picture of fat-footed spiders. Isotopy classes of these spiders form a Teichmüller space and the tools found in Teichmüller theory prove useful in understanding this *Spider Space*. By defining a contracting holomorphic mapping on this spider space, we can iterate this mapping

to a fixed point in Teichmüller space which in turn determines the parameter we seek.

Finally, we extend the results about these polynomial families to the exponential family $E_\lambda(z) = \lambda e^z$. Here, we are able to constructively prove the existence and location of hyperbolic components in the parameter space of E_λ .

Biographical Sketch

David Brown was born in Albany, NY. He spent his secondary school years trying to decide between a career in Chemistry or Mathematics. Not knowing which to choose, he decided to become a chemical engineer. After two years and one internship, he realized how very little he liked the field and dropped out of college. He spent the next four years as a pharmacy manager and an accountant. Finishing his Bachelor's degree as a part-time student at Ithaca College, he decided to go to graduate school at Cornell and finally fulfill the desire to work in mathematics. A little while later, he became a student of John Hubbard and really learned what it means to study mathematics.

While finishing his undergraduate degree, David met his future wife Amy. They were married in the winter of 1995 and had their first child, Jake, four years later. Life is still unfolding and David hopes that he keeps taking the interesting turns that the early part of his life has taken.

to Amy and Jake

Acknowledgements

First and foremost, my deepest thanks must go to my advisor, John H. Hubbard. He was kind enough to take me on as a student when I made a last minute change in advisors. More than just taking me on as a student, he gave me a problem that used in an important way the area of my previous studies.

I really benefited from John's approach to advising, which is much more collaborative than other advisors. I always felt that his suggestions were meant as a guide rather than stone cold fact, and thus, I was able to discover theorems and proofs for myself. This is a beneficial way of learning as it helps to instill confidence in my creative abilities.

Beyond these thesis related ideas, I really became aware of the process of creating mathematics under John's tutelage. I think back to two enjoyable opportunities: a working group in dynamical systems and working on his next text. Both taught me how to think beyond the small pieces and try to grasp an overall picture. It also made me aware of how time-consuming such projects are and how generous John was in sharing his time to discuss ideas.

Outside of mathematics, it was always enjoyable to listen to his stories and opinions. My family and I always felt welcome in the Hubbards' home and enjoyed

very good food and wine there. Also, how many mathematics professors will spend time playing with their advisees infant son? So many thanks go to John and his wife Barbara and children for their hospitality whether in Ithaca or in France.

I also wish to thank the other members of my committee. Cliff Earle introduced me to the beauty of complex analysis and his student Sudeb Mitra taught me the basics of Teichmüller theory. John Smillie provided valuable advice on how to present mathematics at conferences and listened politely as I presented the complaints of graduate students when he served as chair of the department.

I also need to thank Suzanne Hruska, who was a fellow dynamical systems student and helped me remember application dates to conferences. Kathryn Nyman was kind enough to share an office with me for two years and kindly listened to my complaints about Calculus and the job search process. I must also thank the support staff for the mathematics department who made the administrative side of education very easy. These people include Donna Smith, Arletta Havlik, Joy Jones, Michelle Klinger, and Cathy Stevens. I thank my whole family who thought I would be in school forever.

Most of all, I must thank my wife Amy for bearing with me as I attended graduate school. She stuck with me during all the times I questioned whether I made the right decision in going for a PhD. She gave me the peace and sanity I needed and for that I will forever be in her debt. Amy made life easier through her constant support. Finally, I must thank my son Jake for all the smiles and laughs.

Table of Contents

1	Introduction	1
1.1	Organization of the Thesis	8
2	Dynamical Preliminaries	10
2.1	Rational Dynamics	10
2.1.1	Local Picture	10
2.1.2	Global Picture	12
2.1.3	Dynamic Rays	15
2.1.4	Orbit Portraits	17
2.2	Dynamics of $P_{d,\lambda}$	23
2.2.1	Parameter Plane for $P_{d,\lambda}$	24
2.2.2	Parameter Rays	29
2.2.3	Size of B_d	32
3	Analytic Preliminaries	37
3.1	Introduction	37
3.2	Quadratic Differentials	37
3.3	Schwarzian Derivative	39
3.4	Teichmüller Theory	43
3.4.1	Quasiconformal Mappings	43
3.4.2	Classical Teichmüller Space	44
3.5	Holomorphic Motions	46
4	Spider Space and the Spider Map	48
4.1	Standard Clubbed Spider	49
4.1.1	The Looping Number	49
4.1.2	A Kneading Sequence	52
4.2	Spider Space	53
4.3	Spider Mappings	54
4.3.1	Defining the Final Leg and Final Foot	55

4.4	Characterization of Spider Maps	59
4.5	Fixed Points of Spider Maps	61
5	Complex Analytic Structure of Spider Space	63
5.1	Analytic Structure of Spider Space	63
5.2	The Tangent Space to Spider Space	65
6	Contraction of the Spider Map	69
6.1	The Push-forward Operator	69
6.2	Derivative of the Spider Map	72
6.3	Convergence of the Algorithm	74
7	Extension to Exponentials	83
7.1	Introduction	83
7.2	Exponential Dynamics	83
7.2.1	Hairs in the Dynamical Plane	85
7.2.2	Hyperbolic Components in Parameter Plane	87
7.3	Exponential Kneading Sequence	89
7.4	Exponential Spider Space	95
7.5	Exponential Spider Mapping	98
7.5.1	Fixed Point of Exponential Spider Mapping	100
7.5.2	Convergence to a Fixed Point	101
	Bibliography	104

List of Figures

1.1	The bifurcation diagram for $z \mapsto \lambda \left(1 + \frac{z}{3}\right)^3$ with parameter rays indicated.	6
1.2	Fixed spider in the filled-in Julia set of $P_{3,\lambda}$ with $\lambda \approx -0.0394 + 1.5i$	7
2.1	The Julia and filled-in Julia sets for $z \mapsto z^2 - 1$	14
2.2	Julia and filled Julia sets for $z \mapsto z^2 + 0.278125 + 0.529375i$	15
2.3	J_P for $P(z) = z^3 + 0.155 + 1.025i$ along with dynamic rays.	18
2.4	Julia set for $z \mapsto z^2 - 1.25$, showing the four rays landing at a period two parabolic cycle.	19
2.5	Julia set for $z \mapsto z^2 + c$, with $c \approx -0.1571 + 1.0327i$. Shown are the four pairs of rays landing on the repelling periodic orbit on the boundaries of the Fatou components containing the attracting cycle.	20
2.6	Julia set for $z \mapsto z^2 + c$, with $c \approx -1.1343 + 0.2353i$, showing the six rays landing at a period two repelling orbit.	21
2.7	Schematics for the orbit portraits associated with Figures 2.4 , 2.5, 2.6.	22
2.8	The bifurcation diagram B_3	24
2.9	The bifurcation diagram B_4	24
2.10	The bifurcation diagram B_8	25
2.11	The bifurcation diagram B_{20}	25
2.12	The bifurcation diagram B_3 and some parameter rays.	33
2.13	The bifurcation diagram B_4 and some parameter rays.	33
4.1	Standard spider for $\theta = \frac{3}{15}, \mu = 0.5i, d = 2$	50
4.2	Looping numbers. The left picture has $\alpha(\Gamma) = +\frac{5\pi}{2}$ and $\ell = +1$. The right picture has $\alpha(\Gamma) = -\frac{3\pi}{2}$ and $\ell = 0$	51
4.3	Some typical spiders for a period 4 cycle.	54
4.4	The orbit portrait for $\theta = \frac{4}{80}$ and $d = 3$	57
4.5	Demonstration of the trimming process.	58
4.6	Spider map for $d = 2, \theta = \frac{3}{15}, \mu = 0.5i$	59

7.1	The parameter plane for $E_\lambda(z) = \lambda e^z$	87
7.2	Standard Exponential Spider with external address $\overline{0102}$	97

Chapter 1

Introduction

Holomorphic dynamical systems contain structures which are understood through a rich interplay between complex analysis, combinatorics, and topology. One such structure is the Mandelbrot set, which was probably the most widely recognizable mathematical object of the twentieth century. Since the first pictures of the Mandelbrot set appeared twenty-five years ago, many people have studied various aspects of this set and continue to this day to discover new problems related to it ([20]). To this day, the main open conjecture is the local connectivity of the Mandelbrot set. The most satisfying treatise on complex dynamics is the Orsay notes of Douady and Hubbard [9]. In these notes, we see the roots of the interplay between various fields in trying to understand the Mandelbrot set.

One important question related to the Mandelbrot set is the question of which rays land, and where these rays land? Unless you are Douady or Hubbard, this can sometimes be a challenge to determine landing points. Thus, different techniques have been developed to answer this question. For instance, the internal addresses

described by Schleicher [29] give a very elegant method of relating external angles to kneading sequences of hyperbolic components. A different point of view and answer can be found in the Spider algorithm in [15]. Given a rational angle θ , the Spider algorithm produces a sequence of parameters that converges to a Misiurewicz point or the center of a hyperbolic component at which the external ray \mathcal{R}_θ lands. Thus, the Spider algorithm identifies hyperbolic components by locating the unique parameter c for which the critical orbit is periodic and has assigned combinatorics in the sense that the dynamic ray of angle θ lands at the boundary of the Fatou component containing the critical value. A natural extension of the Spider algorithm is an algorithm which converges to the other parameters inside the hyperbolic component determined by θ . We now make this more precise.

Let W be the hyperbolic component of the Mandelbrot set determined by θ and let \mathbb{D} denote the open unit disc. Recall that there is an analytic isomorphism $\chi : W \rightarrow \mathbb{D}$ given by $\chi(c) = (P_c^{\circ N})'(z_0)$, where z_0 is any of the points of the unique attracting cycle for $P_c(z) = z^2 + c$. So, by specifying $\theta \in \mathbb{Q}/\mathbb{Z}$ and a complex number μ satisfying $0 < |\mu| < 1$, is there a method for determining the parameter c and the periodic point z_0 ? By modifying the Spider algorithm, it is possible to determine this information. In fact, this modified Spider algorithm simultaneously finds this parameter and a parameterization of the linearizing neighborhood of the attracting periodic cycle. In particular, the algorithm produces two sequences of complex numbers: the first sequence converges to the correct parameter and the second converges to one of the points of the unique attracting cycle for $z \mapsto z^2 + c$.

In fact, we will describe this modified Spider algorithm in the more general setting

of unicritical polynomials of arbitrary degree, working with the family of polynomials $P_{d,\lambda}(z) = \lambda(1 + \frac{z}{d})^d$ and their bifurcation diagrams, B_d . Since these polynomials are affine conjugate to the polynomials $Q_{d,c}(z) = z^d + c$, we can transfer the results back to the bifurcation diagrams for $Q_{d,c}$ (known as Multibrot sets.) The reason we work with $P_{d,\lambda}$ is that these polynomials converge dynamically to the family $E_\lambda(z) = \lambda e^z$. Hence, the modified Spider algorithms for the polynomial families can be generalized to the infinite degree case. These spider algorithms are versions of Thurston's algorithm as explained in [10].

Working in arbitrary degrees introduces some added difficulties, most notably the fact that for $d \geq 3$, $\chi : W \rightarrow \mathbb{D}$ is not an analytic isomorphism, but rather a $d - 1$ covering map. Hence, we must identify $d - 1$ parameters in each hyperbolic component and have a way of distinguishing these parameters. So, we must solve the following:

Question 1. *Let $d \geq 2$ be an integer, $\theta \in \mathbb{R}/\mathbb{Z}$ periodic under $\theta \mapsto d\theta$ of period N , and $\mu \in \{z \in \mathbb{C} : 0 < |z| < 1\}$. With this data, can we locate the parameters λ such that $P_{\lambda,d}(z) = \lambda(1 + \frac{z}{d})^d$ has an attracting cycle of length N with multiplier μ ?*

The following results from Chapter Six answer this question affirmatively.

Theorem 6.3.7 *Suppose that θ is periodic under $\theta \mapsto d\theta$ and that $0 < |\mu| < 1$. Then, the spider mapping on spider space has a unique fixed point which can be found under iteration.*

and

Corollary 6.3.8 *With θ, μ as in Theorem 6.3.7, there exist $d - 1$ polynomials $P_{\lambda,d}(z) = \lambda(1 + \frac{z}{d})^d$ such that $P_{\lambda,d}$ has an (attracting) cycle of length equal to the*

period of θ with multiplier μ , and having the specified combinatorics from θ .

However, the true power of Spider Theory is realized when we extend the algorithm to work for the exponential family $E_\lambda(z) = \lambda e^z$. It has been conjectured for the past 20 years that the hyperbolic components of the parameter space for the exponential family exist and are encoded by external addresses. The difficulty in proving their existence is the lack of a center for these components. The typical method of locating the center of a hyperbolic component (where the map is post-critically finite) cannot work for exponential maps as there are no critical points and the singular value can never be periodic.

Hence, the work in the early chapters is a prelude to the following application of Spider theory to exponentials. The construction of Spider Space in the polynomial case is as general as possible so that only slight modifications are needed to create Exponential Spider Space and Spider mappings on that space. The main results are **Theorem 7.5.4** *The exponential spider mapping has a unique fixed point $[\varphi_\infty]$ which is found under iteration of the spider mapping.*

and

Theorem 7.5.5 *For any $N \geq 3$ and any bounded periodic external address $\theta = s_0 s_1 \dots$, there is a hyperbolic component W in the parameter space for $E_\lambda(z)$ such that for each $\lambda \in W$, the hair $h_{\lambda, \theta}$ lands at the characteristic repelling periodic point on the boundary of the Fatou component containing 0. Any such hyperbolic component is uniquely specified by the sequence θ .*

Results concerning the existence of hyperbolic components of the exponential family have been recently announced by Devaney, Jarque, and Fagella ([11]) and

Schleicher ([31]). Our result gives existence and uniqueness of the coding of the components and allows us to locate the positions of attracting parameters anywhere in parameter space.

Finally, the Spider algorithm defined in this thesis is a version of Thurston's algorithm as mentioned earlier with the major difference being that our maps are not post-critically finite. Most work done with Thurston-type algorithms of this nature have relied on this finiteness of the critical orbit. In a preprint, Jiang, Cui, and Sullivan ([6]) have also announced a Thurston algorithm for geometrically finite rational maps which are not post-critically finite.

The Spider algorithm is a simplified version of Thurston's topological characterization of rational mappings [10] and the underlying technique used is iteration on an appropriate Teichmüller space. The idea of iteration on Teichmüller spaces goes back to Thurston. In fact, two very important theorems rely on this technique: the topological characterization of rational mappings and the hyperbolization of 3-manifolds. A detailed discussion of these theorems and the background information can be found in a paper by McMullen [25] and a forthcoming manuscript by Hubbard [14].

In answering Question 1, we will also create an iteration on a Teichmüller space, but in contrast to the above theorems, this Teichmüller space is infinite dimensional and hence produces many challenges not found in the original Spider algorithm.

The following example illustrates the motivation behind the description of the modified Spider algorithm. Consider the polynomial $P_\lambda(z) = \lambda \left(1 + \frac{z}{3}\right)^3$, with $\lambda \approx -0.0394 + 1.5i$. This polynomial has an attracting cycle of length 3 with multiplier

$\mu = 0.8$ and the parameter λ lies in the hyperbolic component of B_3 encoded by the parameter ray $\mathcal{R}_{2\theta}$ where $\theta = 1/26$. See Figure 1.1.

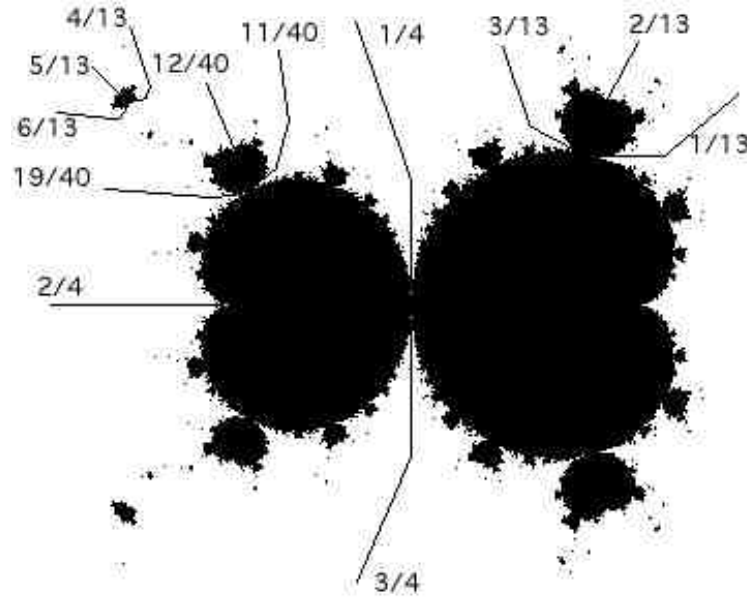


Figure 1.1: The bifurcation diagram for $z \mapsto \lambda \left(1 + \frac{z}{3}\right)^3$ with parameter rays indicated.

By a theorem of Koenigs (Theorem 2.1.1), there is a neighborhood U of the attracting cycle such that $P_\lambda^{\circ 3}$ is conformally conjugate to multiplication by μ . That is, there is a conformal map $\varphi : U \rightarrow \mathbb{D}$ such that $\varphi \circ P_\lambda^{\circ 3} \circ \varphi^{-1}(z) = \mu z$. The domains U , $P_{d,\lambda}(U)$, and $P_{d,\lambda}^{\circ 2}(U)$ form the feet of a spider and its legs approximate the indicated dynamic rays landing at the repelling fixed point in the boundary of the Fatou components containing the critical orbit. See Figure 1.2.

This example serves as the prototype for the (fat-footed) Spiders we define in Chapter 3. Using combinatorial information coming from the angle θ and the analytic information of the multiplier μ , we construct a space of univalent mappings,

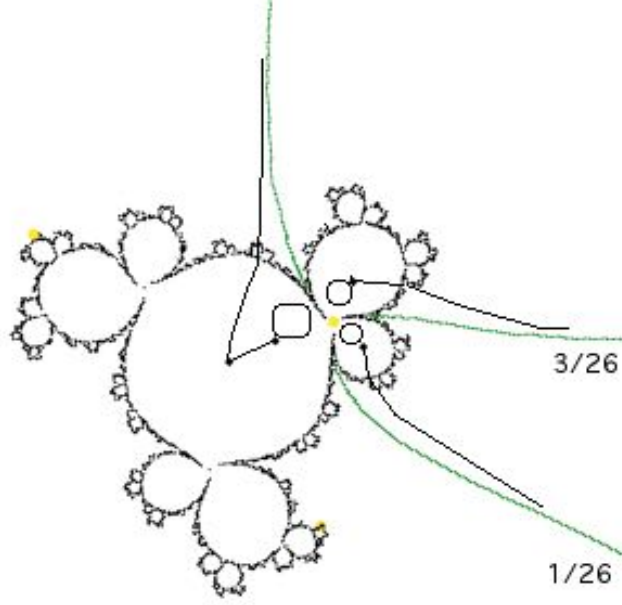


Figure 1.2: Fixed spider in the filled-in Julia set of $P_{3,\lambda}$ with $\lambda \approx -0.0394 + 1.5i$.

called Spider Space. Since the image of a univalent mapping determines the mapping, there is a concrete visualization of these mappings in which they closely resemble spiders with long legs and fat feet.

Let z_0 be the periodic point in the connected component of the Fatou set that contains 0 and let $z_1 = P_\lambda(z_0)$ and $z_2 = P_\lambda(z_1)$. Let U_0 be a linearizing neighborhood of z_0 which contains 0 on the boundary and set $U_1 = P_\lambda(U_0)$ and $U_2 = P_\lambda(U_1)$. These neighborhoods serve as the feet of a spider. To define the legs of the spider, let γ_0 be any continuous curve that connects 0 to ∞ and agrees with the dynamic ray \mathcal{R}_θ near infinity; set $\gamma_1 = P_\lambda(\gamma_0)$ and $\gamma_2 = P_\lambda(\gamma_1)$. See Figure 1.2. Then, $\bigcup_{j=0}^2(\overline{U}_j \cup \gamma_j)$ forms a spider for this mapping; we think of $\{\infty\}$ as a small body.

Now, the key characteristic of such a spider is that it is invariant under P_λ^{-1}

in the following sense. Let \tilde{U}_0 be the pre-image of U_1 that has 0 on its boundary and let $\tilde{\gamma}_0$ be the pre-image of γ_1 which leads to 0. Similarly, denote by \tilde{U}_1 the pre-image of U_2 containing $\lambda = P_\lambda(0)$ and let $\tilde{\gamma}_1$ is the pre-image of γ_2 leading to λ . Finally, \tilde{U}_2 will consist of the pre-image of U_0 containing $P_\lambda(\lambda)$ and restricted to the subdisc containing $P_\lambda(\lambda)$ on its boundary. Note that this new spider is isotopic to the old spider relative to the feet. Hence, we have a fixed point in the Spider Space of isotopic spiders under the mapping defined by taking inverse branches of P_λ . This mapping is called a Spider mapping. From this example, we create a general algorithm which converges under iteration to the parameterization we seek.

1.1 Organization of the Thesis

The basic theory of the iteration of holomorphic mappings is presented in Chapter 2. By now, this material is well-known and many references on the subject exist, including but not limited to [9],[21], [7], and [32]. After a general introduction, the focus switches to the polynomial family $P_{d,\lambda}(z) = \lambda \left(1 + \frac{z}{d}\right)^d$. In particular, we describe the structure of parameter space that will be needed for the modified Spider algorithm.

In Chapter 3, we present the necessary background from complex analysis, especially that of Teichmüller spaces. While this chapter could possibly be developed and interwoven in the text as needed, it serves as a contrast to the more intuitive Teichmüller space used in the thesis.

The bulk of the results begin with Chapter 4, in which we define Spider Space as a space of univalent mappings defined using the data θ and μ . In the same chapter,

Spider mappings are defined as branches of the inverse to $P_{d,\lambda}$. The modified Spider algorithm is the iteration of a Spider mapping and we show that a fixed point of a spider mapping produces the parameterization of the attracting cycle sought in Question 1. As it turns out, for each Spider Space, there are infinitely many spider mappings defined and we classify them into finitely many distinct classes. In fact, we show that there are $d - 1$ classes of spider mappings and each class determines a unique parameter that answers Question 1.

In Chapter 5, Spider Space is shown to be isomorphic to a classical infinite dimensional Teichmüller space and hence has the structure of an analytic Banach manifold. We also identify the tangent space to Spider Space.

In Chapter 6, we prove the modified Spider algorithm converges to a fixed spider. We show that the derivative of the spider mapping is strictly contracting with respect to a norm on the tangent space to Spider Space, which, combined with an invariant subspace of spiders, allows us to iterate to a fixed point of the spider mapping starting with an arbitrary point of Spider Space. The main results concerning polynomials are proved in Chapter 6. The dynamics of the exponential family and the Exponential Spider algorithm in the periodic case are discussed in Chapter 7.

Chapter 2

Dynamical Preliminaries

In this chapter, we gather the main results from the iteration of holomorphic mappings of the Riemann sphere that will be used in this thesis. We begin with rational dynamics, in particular, focusing on the dynamics of polynomials. These are now classical results and most proofs will be omitted. Sketches of proofs will appear where such arguments illuminate the ideas found later in this work.

2.1 Rational Dynamics

2.1.1 Local Picture

Consider the mapping

$$f(z) = \mu z + a_2 z^2 + a_3 z^3 + \dots$$

holomorphic in a neighborhood of the origin, having $z = 0$ as fixed point and $\mu = f'(0)$ as *multiplier*. The following result, due to Koenigs, is central to the

iteration of holomorphic mappings.

Theorem 2.1.1. (Linearization) *If the multiplier μ satisfies $|\mu| \neq 0, 1$ then there exists an injective holomorphic mapping φ defined in a neighborhood of the origin, so that $(\varphi^{-1} \circ f \circ \varphi)(z) = \mu z$. Furthermore, φ is unique up to multiplication by a nonzero constant.*

Proof. See [21] . □

The map φ is called the *linearizing map* at the fixed point 0. Often, we normalize the linearizing map by assuming that $\varphi'(0) = 1$. A fixed point is called *attracting* if $|\mu| < 1$ and *repelling* if $|\mu| > 1$.

Of course, we transfer this result to any fixed point in the plane. Thus, we get a very nice local picture in which points in a neighborhood of an attracting fixed point tend to this fixed point under successive iteration of our mapping. This thesis will focus on the study of attracting periodic points and their linearizing maps.

Now, we consider the two cases not covered by the Koenigs' theorem. In the case $|\mu| = 1$, we say that the origin is an *indifferent* fixed point. Here the local situation is rather complicated. If $\mu = e^{2\pi i\theta}$, where $\theta \in \mathbb{R}/\mathbb{Z}$, then the fixed point is called *parabolic* and f is linearizable (in the same sense as in Theorem 2.1.1) if and only if θ satisfies a precise number theoretic condition. The theory of indifferent fixed points is used very little in this thesis and so we say nothing more here on this very interesting topic.

Finally, we also have the case in which $\mu = 0$. In this case, we say that f has a *superattracting* fixed point at the origin. There is a smallest $k > 1$ such that

$$f(z) = a_k z^k + a_{k+1} z^{k+1} + \dots$$

where $a_k \neq 0$. It is easy to see that locally, f is a map of degree k . Thus, it is natural to attempt to conjugate f to the map $z \rightarrow z^k$. This is precisely what Böttcher's theorem states is true.

Theorem 2.1.2. (Böttcher's Theorem) *Suppose that*

$$f(z) = a_k z^k + a_{k+1} z^{k+1} + \dots,$$

where $k \geq 2$ and $a_k \neq 0$. Then, there is an injective holomorphic mapping φ defined in a neighborhood of the origin, so that $\varphi \circ f \circ \varphi^{-1}(z) = z^k$. Furthermore, φ is unique up to multiplication by a $(k-1)^{\text{st}}$ root of unity.

Note that the same results follow through for periodic points of mappings. In particular, if p is a periodic point of period N , then we define the *multiplier* of the periodic orbit of p to be $\mu = (f^{\circ N})'(p)$. Then, $\mathcal{O} = \{p, f(p), \dots, f^{\circ N}(p)\}$ is an *attracting cycle* for f if $|\mu| < 1$.

2.1.2 Global Picture

The work of Fatou and Julia in the early 20th century led to understanding the global behavior of the iteration of a holomorphic mapping of the Riemann sphere, $\hat{\mathbb{C}} = \mathbb{C} \cup \{\infty\}$. In fact, the sphere breaks up into two complementary subsets: the open Fatou set Ω_f in which orderly dynamics occur, and the Julia set J_f in which the behavior of f is chaotic. Understanding the dynamics of f resides in the topology and geometry of the Julia set and classifying the components of the Fatou set. The most general way of defining the Fatou and Julia sets comes from the theory of normal families.

Definition 2.1.3. (Normal Families)

A family of analytic functions, defined a common domain U , is called a normal family if every sequence in the family contains a subsequence that either converges uniformly on compact subsets of U , or converges uniformly on compact subsets of U to infinity.

Definition 2.1.4. (Fatou and Julia Sets)

A point $z \in \hat{\mathbb{C}}$ belongs to the Fatou set Ω_f if there is a neighborhood U of z on which the sequence of iterates $\{f^{\circ n}\}_{n=0}^{\infty}$ forms a normal family. The Julia set J_f is the complement of Ω_f .

In order to determine the Fatou set, it will be useful to have a criterion for being normal, since the definition of normal family can be difficult to verify.

Theorem 2.1.5. (Montel's Theorem) Let $\{f_\alpha : U \rightarrow \hat{\mathbb{C}}\}_{\alpha \in \mathcal{A}}$ be a family of holomorphic functions on an open set $U \subset \hat{\mathbb{C}}$. If the family $\{f_\alpha\}$ omits at least three values in $\hat{\mathbb{C}}$, then $\{f_\alpha\}$ is normal on U .

We now gather some basics results about Fatou and Julia sets.

Proposition 2.1.6. (Properties of Julia Sets)

1. The Fatou and Julia sets are completely invariant sets. That is, $f(J_f) = J_f$, $f^{-1}(J_f) = J_f$, $f(\Omega_f) = \Omega_f$, $f^{-1}(\Omega_f) = \Omega_f$.
2. J_f is non-empty and perfect. Either it has no interior or it is the entire Riemann sphere.
3. J_f equals the closure of the repelling periodic points.

For the rest of this section, we specialize to the case of the iteration of a polynomial P .

Definition 2.1.7. *The filled-in Julia set of P is the set*

$$K_P = \{z \in \mathbb{C} \mid P^{o_n}(z) \not\rightarrow \infty \text{ as } n \rightarrow \infty\}$$

of points with bounded forward orbits.

This definition fits very naturally with the general theory as the next result indicates.

Proposition 2.1.8. *J_P is the topological boundary of K_P .*

See Figures 2.1 - 2.2 for pictures of Julia sets.

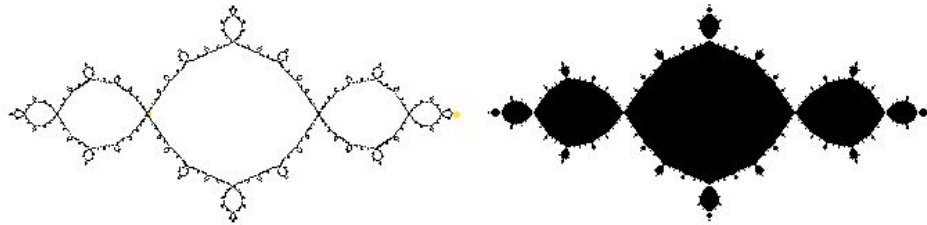


Figure 2.1: The Julia and filled-in Julia sets for $z \mapsto z^2 - 1$.

We now see that critical points play a major role in complex dynamics.

Theorem 2.1.9. (Fatou)

- (a) *All critical points (in \mathbb{C}) of P belong to K_P if and only if K_P is connected.*
- (b) *If no critical point of P lies in K_P , then K_P is a Cantor set and there is a homeomorphism $\phi : K_P \rightarrow \Sigma_d$, where (Σ_d, σ) is the one-sided shift on d symbols, such that $\phi \circ P = \sigma \circ \phi$.*

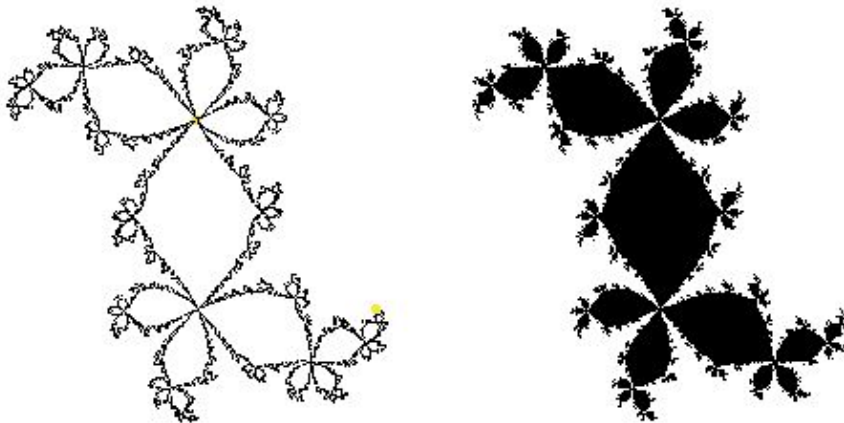


Figure 2.2: Julia and filled Julia sets for $z \mapsto z^2 + 0.278125 + 0.529375i$.

2.1.3 Dynamic Rays

In this section, we will introduce dynamic and parameter rays, which give a beautiful combinatorial description of the dynamic and parameter planes of polynomials. We know [21] that for every parameter $c \in \mathbb{C}$ there is a neighborhood U of infinity and a *Böttcher map* $\phi_c : U \rightarrow U$, fixing infinity, such that $\phi_c \circ Q_{d,c} \circ \phi_c^{-1} = z^d$. This follows from the fact that infinity is always a super-attracting fixed point of any polynomial. Defining a Green's function g_c on U by

$$g_c(z) = \log |\phi_c(z)| \quad \text{for } z \in U,$$

we have the following functional equation

$$g_c(z) = \frac{g_c(Q_{d,c}(z))}{d}.$$

From this, it follows that the Green's function extends continuously to $\hat{\mathbb{C}} - K_{Q_{d,c}}$ and tends to zero as z approaches $K_{Q_{d,c}}$. Hence, we define $g_c(z) := 0$ for $z \in K_{Q_{d,c}}$.

For $t > 0$, the set $\{z \in \mathbb{C} : g_c(z) = t\}$ is called an *equipotential curve of potential t* .

Next, note that g_c has a critical point p whenever p is a critical or precritical point of $Q_{d,c}$; in other words, if $Q_{d,c}^{\circ k}(p) = c$ for some integer $k \geq 1$. If $K_{Q_{d,c}}$ is connected, then the critical point lies in the filled-in Julia set, and hence, g_c has no critical points outside of $K_{Q_{d,c}}$. If $K_{Q_{d,c}}$ is not connected, then g_c has infinitely many critical points. This means that the Böttcher map ϕ_c can be continued analytically when $g_c(z) > g_c(0)$. In particular, this means that if $K_{Q_{d,c}}$ is connected, then ϕ_c extends to a conformal mapping from $\hat{\mathbb{C}} - K_{Q_{d,c}}$ onto $\hat{\mathbb{C}} - \bar{\mathbb{D}}$.

Definition 2.1.10. (Dynamic Rays)

Let c be a parameter for which $K_{Q_{d,c}}$ is connected. The dynamic ray of angle θ is the set $\mathcal{R}_\theta = \{\phi_c^{-1}(re^{2\pi i\theta}) : r > 1\}$.

If the limit

$$\lim_{r \searrow 1} \phi_c^{-1}(re^{2\pi i\theta})$$

exists, then we say that the ray \mathcal{R}_θ *lands* at its limit point. A ray \mathcal{R}_θ is called *periodic* if the angle θ is periodic under multiplication by d .

The following result is due to Sullivan, Hubbard, and Douady. See [21].

Theorem 2.1.11. (Periodic Rays Land)

Consider a parameter with a connected Julia set. Then, every periodic and preperiodic dynamic ray lands at a repelling or parabolic point which is periodic or preperiodic, respectively.

We also have

Theorem 2.1.12. *For a connected $K_{Q_{d,c}}$, every periodic or preperiodic repelling or parabolic point in $J_{Q_{d,c}}$ is the landing point of at least one and at most finitely many periodic or preperiodic dynamic rays. Furthermore, if $K_{Q_{d,c}}$ is locally connected, then the number of rays landing at $z \in \partial K_{Q_{d,c}}$ equals the number of components of $K_{Q_{d,c}} - \{z\}$.*

A very important property of dynamic rays is the following.

Lemma 2.1.13. *The dynamic ray \mathcal{R}_θ lands at $z \in \partial K_{Q_{d,c}}$ if and only if $\mathcal{R}_{d\theta}$ lands at $Q_{d,c}(z)$.*

This lemma and the previous theorems show that there is a notion of periodicity of rays landing at a repelling or periodic point. Let \mathcal{O} be a repelling or parabolic periodic orbit and let \mathcal{R}_θ be a dynamic ray landing at one of the points of the orbit. It is possible for the period of the orbit and the period of the angle θ to be different. For example, in Figure 2.3 the θ has period two while the ray \mathcal{R}_θ lands at a fixed point in the Julia set. We define the *ray period of \mathcal{O}* to be the period of the angle θ .

2.1.4 Orbit Portraits

In this section, we introduce *orbit portraits*, which we use in defining spider mappings. A similar treatment of orbit portraits may be found in [22] or [12]. Orbit portraits give a combinatorial description of Julia sets and are used to study the landing properties of rays in the parameter plane. We will use them to show us where to look for the critical orbit of a mapping with an attracting cycle. We have in mind the polynomials $f_c(z) = z^d + c$, with $d \geq 2$, when defining orbit portraits,

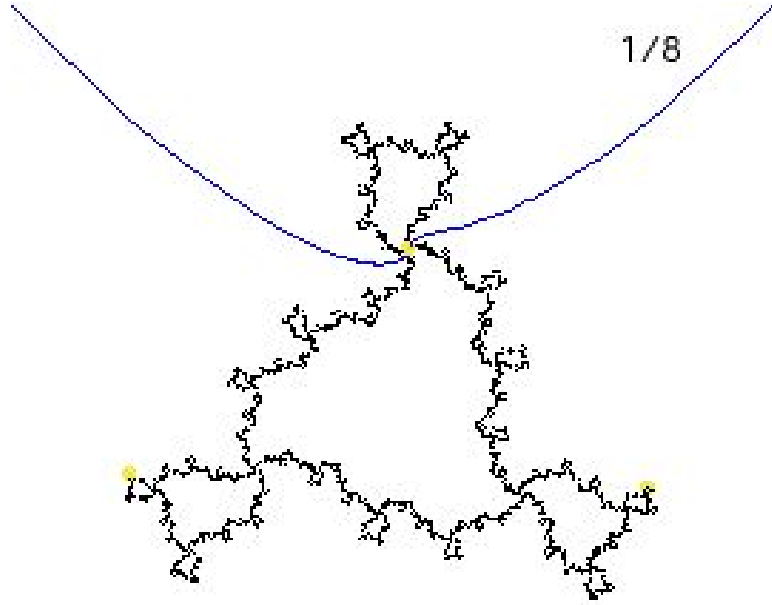


Figure 2.3: J_P for $P(z) = z^3 + 0.155 + 1.025i$ along with dynamic rays.

but the exposition works just as well for the polynomials $z \mapsto \lambda \left(1 + \frac{z}{d}\right)^d$. Figures 2.4 and 2.6 show rays landing on the Julia sets of quadratic polynomials. Later, we will draw a caricature of the landing pattern using orbit portraits.

Definition 2.1.14. (Orbit Portraits)

Let A_i be the set of angles for a periodic orbit $\mathcal{O} = \{z_1, \dots, z_N\}$ of f_c for which the dynamic rays of angles $\theta \in A_i$ land at z_i . The set $\mathcal{P} = \{A_1, \dots, A_N\}$ is called the orbit portrait of \mathcal{O} with respect to f_c .

A portrait $\mathcal{P} = \{A_1, \dots, A_N\}$ is called *essential* if each A_i contains at least two angles; otherwise, it is *non-essential*. If the period of all angles in $A_1 \cup \dots \cup A_N$ is equal to N , then the portrait is called *primitive*; otherwise it is *non-primitive*. Note that the condition of being primitive means that the period of the rays and the period of the orbit are the same.

Also note that for $d = 2$, all parabolic parameters have an essential portrait. This is not true for $d > 2$, as there are parabolic parameters at which only one ray lands. See Figure 1.1.

The sets A_1, \dots, A_N are *pairwise unlinked* if, for each $i \neq j$, the sets A_i and A_j are contained in disjoint sub-intervals of \mathbb{R}/\mathbb{Z} .

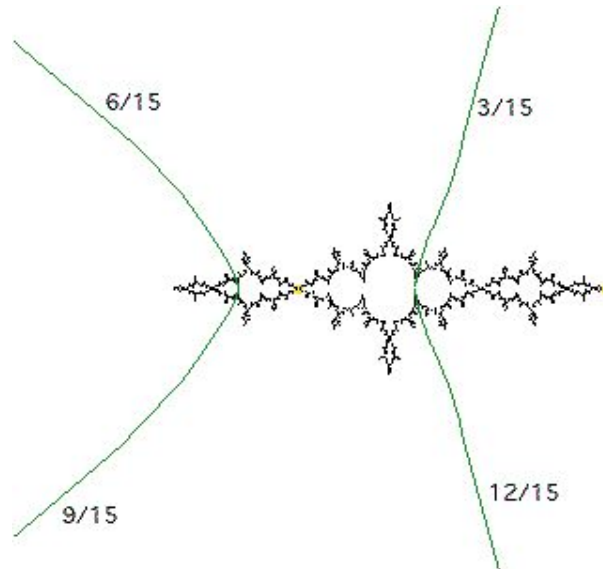


Figure 2.4: Julia set for $z \mapsto z^2 - 1.25$, showing the four rays landing at a period two parabolic cycle.

For example, Figure 2.4 shows a parabolic orbit of period two and ray period four. The associated orbit portrait is

$$\mathcal{P} = \left\{ \left\{ \frac{6}{15}, \frac{9}{15} \right\}, \left\{ \frac{3}{15}, \frac{12}{15} \right\} \right\}.$$

Figure 2.5 shows an orbit of period four and ray period four with

$$\mathcal{P} = \left\{ \left\{ \frac{3}{15}, \frac{4}{15} \right\}, \left\{ \frac{6}{15}, \frac{8}{15} \right\}, \left\{ \frac{12}{15}, \frac{1}{15} \right\}, \left\{ \frac{9}{15}, \frac{2}{15} \right\} \right\},$$

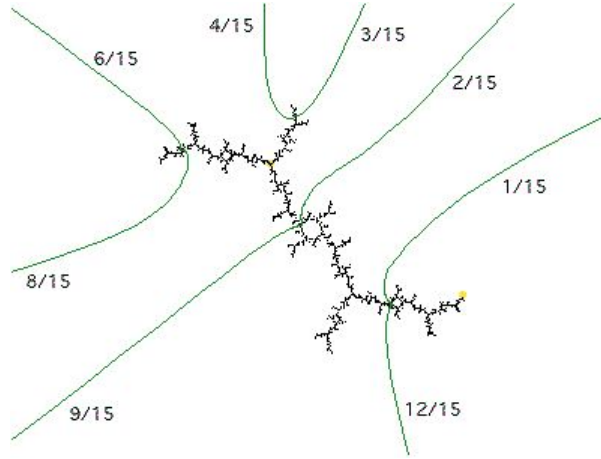


Figure 2.5: Julia set for $z \mapsto z^2 + c$, with $c \approx -0.1571 + 1.0327i$. Shown are the four pairs of rays landing on the repelling periodic orbit on the boundaries of the Fatou components containing the attracting cycle.

and Figure 2.6 shows an orbit of period two and ray period six, with

$$\mathcal{P} = \left\{ \left\{ \frac{22}{63}, \frac{25}{63}, \frac{37}{63} \right\}, \left\{ \frac{11}{63}, \frac{44}{63}, \frac{50}{63} \right\} \right\}.$$

Orbit portraits are characterized by the following properties.

Lemma 2.1.15. (Properties of Portraits)

Let $\mathcal{P} = \{A_1, \dots, A_N\}$ be the orbit portrait of a periodic orbit \mathcal{O} for f_c . Then,

1. Each A_i is a finite subset of \mathbb{Q}/\mathbb{Z} .
2. For each i modulo N , the d -tupling map $t \mapsto dt \pmod{\mathbb{Z}}$ carries A_i bijectively onto A_{i+1} preserving the cyclic ordering on the circle.
3. All angles in $A_1 \cup \dots \cup A_N$ are periodic, of same period, under the d -tupling map.
4. The A_i are pairwise unlinked.

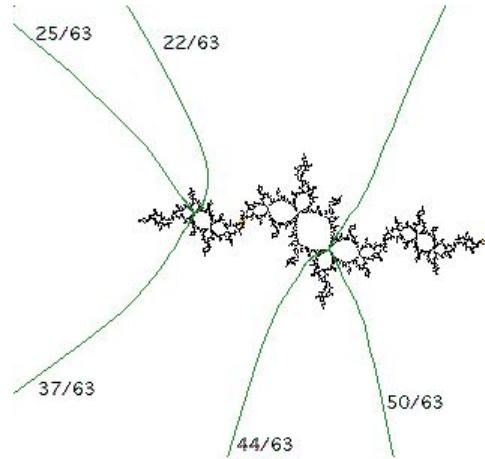


Figure 2.6: Julia set for $z \mapsto z^2 + c$, with $c \approx -1.1343 + 0.2353i$, showing the six rays landing at a period two repelling orbit.

Our interest with orbit portraits lies in knowing what happens to landing patterns in the Julia sets as we perturb a mapping. In visualizing landing patterns of rays, it is useful to give a schematic diagram of the orbit portrait.

We can compactify the plane by adding the circle $\{e^{2\pi it} \infty : t \in \mathbb{R}\}$ at infinity. Inside of this closed (topological) disc, we can form the *diagram* \mathcal{D} and illustrate the orbit portrait \mathcal{P} by drawing all the rays joining \mathcal{O} to the circle at infinity. These rays will be disjoint, except each point in \mathcal{O} is a common endpoint of rays. Figure 2.7 shows various schematic diagrams. Of fundamental importance is the fact that the diagram \mathcal{D} deforms continuously, and thus preserves its topology, as we move the parameter c , as long as the orbit \mathcal{O} remains repelling. This stability follows from the following result.

Lemma 2.1.16. *Let c_0 be a parameter and z_0 a periodic point of f_{c_0} of exact period N such that the multiplier $\mu(c_0, z_0) \neq 1$. Then, there is a neighborhood U of c_0 and a holomorphic function $z : U \rightarrow \mathbb{C}$ such that $z(c)$ is a periodic point of f_c of exact period N for each $c \in U$ and $z(c_0) = z_0$.*

Proof. Let $g(c, z) = f_c^{\circ N}(z) - z$. Clearly, g is holomorphic in c and z and has a zero at (c_0, z_0) . Further, $\frac{d}{dz}g(c_0, z_0) \neq 0$ since $\mu(c_0, z_0) \neq 1$. Thus, the Implicit Function Theorem implies that there are neighborhoods U of c_0 and V of z_0 and a holomorphic function $z : U \rightarrow V$ such that $g(c, z(c)) = 0$. That is, $z(c)$ is periodic of exact period N for $c \in U$. \square

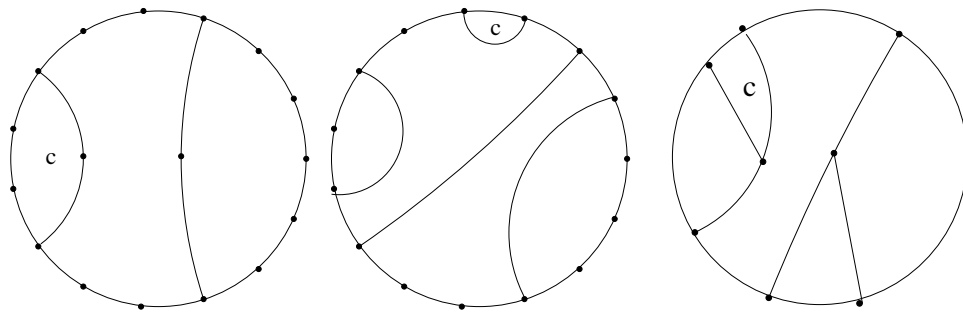


Figure 2.7: Schematics for the orbit portraits associated with Figures 2.4 , 2.5, 2.6.

In Chapter Four, we analyze orbit portraits in terms of the lengths of the arcs that the rays make with the circle at infinity. We make this notion precise here. First, as is usual in holomorphic dynamics, we measure angles in terms of fractions of a full turn. Thus, angles are elements of $\mathbb{R}/\mathbb{Z} \cong \mathbb{S}^1$. Further, since $\mathbb{S}^1 \cong [0, 1)$, the quantity $e^{2\pi i\theta}$, for $\theta \in \mathbb{S}^1$, has a well-defined meaning. Next, we define intervals on \mathbb{S}^1 . Let $\theta_1, \theta_2 \in \mathbb{S}^1$ and define (θ_1, θ_2) to be the open connected component of $\mathbb{S}^1 - \{\theta_1, \theta_2\}$ composed of angles we reach as we travel from θ_1 to θ_2 in a positive

direction. We write $\theta_i < \theta_j < \theta_k$ if $\theta_j \in (\theta_i, \theta_k)$. Finally, the length of an interval $I \subset \mathbb{S}^1$ is denoted by $\ell(I)$, where $\ell(\mathbb{S}^1) = 1$.

Definition 2.1.17. (Complementary Arcs)

Let $A = \{\theta_1, \dots, \theta_k\}$ be an element of orbit portrait \mathcal{P} , with $\theta_1 < \theta_2 < \dots < \theta_k < \theta_1$.

We call the intervals $(\theta_1, \theta_2), (\theta_2, \theta_3), \dots, (\theta_k, \theta_1)$ the complementary arcs for A .

Lemma 2.1.18. *Let \mathcal{P} be an essential orbit portrait. For any $A_i \in \mathcal{P}$, all but one complementary arc for A_i is carried diffeomorphically by the d -tupling map onto a complementary arc for A_{i+1} . The remaining complementary arc for A_i has length greater than $1 - 1/d$ and its image under the d -tupling map covers one particular complementary arc for A_{i+1} d times.*

Proof. Let $I \subset \mathbb{S}^1$ be a complementary arc for A_i of length less than $1/d$. By part (2) of Lemma 2.1.15, the d -tupling map carries I bijectively onto an arc dI of length $d\ell(I)$, bounded by two points of A_{i+1} . Since the cyclic ordering is preserved under the d -tupling map, this image arc does not contain any other point of A_{i+1} . Hence, the image arcs cannot overlap.

□

2.2 Dynamics of $P_{d,\lambda}$

In this section, we discuss the dynamics of the mappings $P_{d,\lambda}(z) = \lambda \left(1 + \frac{z}{d}\right)^d$ for $\lambda \in \mathbb{C}$. In particular, we analyze the bifurcation diagram B_d for $P_{d,\lambda}$. Figures 2.8-2.11 display B_d for various d .

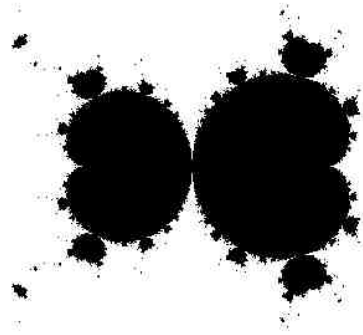


Figure 2.8: The bifurcation diagram B_3 .

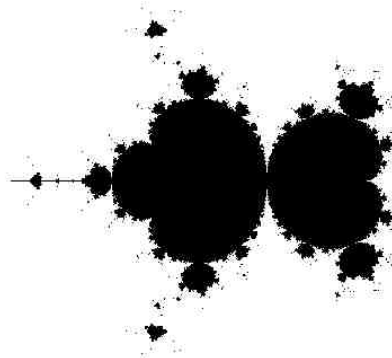


Figure 2.9: The bifurcation diagram B_4 .

2.2.1 Parameter Plane for $P_{d,\lambda}$

First, we describe some of the properties of the parameter plane for the family $P_{d,\lambda}$. We will also indicate the relationship with the parameter plane for the exponential family. The d^{th} bifurcation set, B_d , is the set of parameters λ for which the orbit $P_{d,\lambda}^n(0)$ is bounded. Recall the following fact.

Theorem 2.2.1. *If $\lambda \in B_d$, then the filled-in Julia set $K_{d,\lambda}$ of $P_{d,\lambda}$ is connected. Otherwise, $K_{d,\lambda}$ is homeomorphic to a Cantor set.*

Proof. This follows immediately from Theorem 2.1.9 since each $P_{d,\lambda}$ has only one

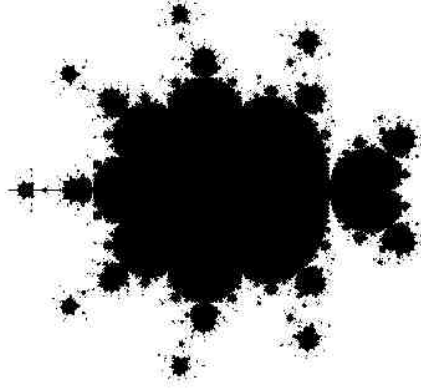


Figure 2.10: The bifurcation diagram B_8 .

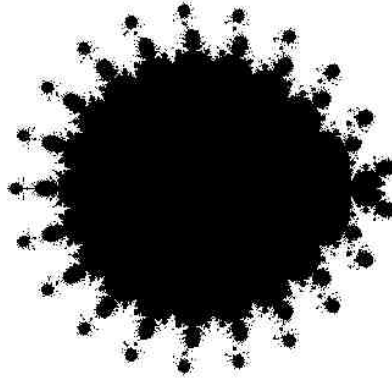


Figure 2.11: The bifurcation diagram B_{20} .

critical point in the plane. □

We now describe the components of B_d .

Definition 2.2.2. *A polynomial or entire mapping is hyperbolic if every critical point is attracted by an attracting periodic cycle.*

Definition 2.2.3. *A component W of the interior of B_d is called a hyperbolic component if $P_{d,\lambda}$ is hyperbolic for some, and hence all $\lambda \in W$. We say that a*

hyperbolic component W has period N if $P_{d,\lambda}$ has an attracting cycle of period N for $\lambda \in W$.

Set

$$C_N^d = \{\lambda \mid P_{d,\lambda} \text{ has an attracting cycle of period } N\}$$

and

$$C_N = \{\lambda \mid E_\lambda \text{ has an attracting cycle of period } N\}.$$

Lemma 2.2.4. *Let W be a connected component of C_N^d . Then W is an open subset of B_d and there is an analytic map $z : W \rightarrow \mathbb{C}$ such that $z(\lambda)$ is an attracting periodic point of period N , for all $\lambda \in W$.*

Proof. By definition, there is a $\lambda_0 \in W$ with an attracting orbit of period N . Since $P_{d,\lambda}$ has only one critical point, it follows that P_{d,λ_0} has a unique attracting orbit of period N . By the analytic dependence of parameters on the multiplier, there is a map $z : W \rightarrow \mathbb{C}$ with $z(\lambda)$ having an attracting cycle of period N . Also, this same lemma shows that every $\lambda \in W$ has a neighborhood U such that all $\lambda \in U$ are hyperbolic. Hence, W is open. Finally, if $P_{d,\lambda}$ has an attracting orbit, then the orbit of the critical point is in the basin of attraction and hence the orbit of the critical point is bounded. Thus, $\lambda \in B_d$. So, $W \subset B_d$. \square

From the above proof, we see that for a given d and $\lambda \in C_N^d$, the critical point $-d$ lies in a component of the basin of attraction of this cycle which contains one point, denoted $z_0 = z_0(\lambda)$, of the attracting cycle. Set $z_i(\lambda) = P_{d,\lambda}^i(z_0)$, for $i = 1, \dots, N-1$. Then, we define the *eigenvalue map*

$$\chi_d : C_N^d \rightarrow \mathbb{D} \quad \text{by} \quad \chi_d(\lambda) = (P_{d,\lambda}^N)'(z_0) = \prod_{i=0}^{N-1} P'(z_i), \quad (2.1)$$

where \mathbb{D} denotes the open unit disc. This map is clearly analytic since $z_0(\lambda)$ varies analytically with λ .

Proposition 2.2.5. (Multiplier Map)

1. C_1^d is bounded by a cardioid-like curve and $\chi_d^{-1} : \mathbb{D} \rightarrow C_1^d$ is an analytic homeomorphism which extends to a homeomorphism $\overline{\mathbb{D}} \rightarrow \overline{C_1^d}$.
2. $\lim_{d \rightarrow \infty} \chi_d^{-1} = \chi^{-1} : \mathbb{D} \rightarrow C_1$ where $\chi^{-1}(\mu) = \mu e^{-\mu}$ and χ is the multiplier map for the exponential family.

Proof. Note that $\lambda \in C_1^d$ and $\chi_d(\lambda) = \mu$ imply

$$\lambda \left(1 + \frac{z}{d}\right)^d \quad \text{and} \quad \lambda \left(1 + \frac{z}{d}\right)^{d-1} = \mu.$$

Thus,

$$\mu = \frac{z}{1 + z/d} \quad \text{or} \quad z = \frac{\mu}{1 - \mu/d}$$

and hence

$$\lambda = \chi_d^{-1}(\mu) = \frac{\mu}{\left(1 + \frac{\mu}{d-\mu}\right)^{d-1}}$$

is an inverse for χ_d . As indicated earlier, χ_d is analytic.

The multiplier map χ_d extends continuously to the boundary of C_1^d to a map $\overline{\chi}_d : \overline{C_1^d} \rightarrow \overline{\mathbb{D}}$. If $\lambda \in \partial \overline{C_1^d}$, then $P_{d,\lambda}$ has a fixed point z_λ with derivative of modulus 1, and $\overline{\chi}_d(z_\lambda) = P'_{d,\lambda}(z_\lambda)$. So, χ_d^{-1} extends continuously to an inverse $\overline{\chi}_d^{-1}$ of $\overline{\chi}_d$. Hence, $\overline{\chi}_d^{-1}$ is a homeomorphism.

In order to prove the second statement, set $\mu = r e^{i\theta} \in \overline{\mathbb{D}}$ and choose a branch of

the logarithm defined on $\mathbb{C} - \{x \leq 0\}$. Then,

$$\begin{aligned}
\lim_{d \rightarrow \infty} \log \left(1 + \frac{\mu}{d - \mu} \right)^{d-1} &= \lim_{d \rightarrow \infty} (d-1) \log \left(\frac{d}{d - \mu} \right) \\
&= \lim_{d \rightarrow \infty} (d-1) \left[\log d - \frac{1}{2} \log(d^2 - 2rd \cos \theta + r^2) \right] \\
&\quad + i \lim_{d \rightarrow \infty} (d-1) \frac{r \sin \theta}{d - r \cos \theta} \\
&= r \cos \theta + ir \sin \theta \\
&= \mu.
\end{aligned}$$

Thus,

$$\lim_{d \rightarrow \infty} \left(1 + \frac{\mu}{d - \mu} \right)^{d-1} = e^\mu$$

and hence

$$\lim_{d \rightarrow \infty} \chi_d^{-1}(\mu) = \lim_{d \rightarrow \infty} \frac{\mu}{\left(1 + \frac{\mu}{d - \mu} \right)^{d-1}} = \mu e^{-\mu}.$$

□

Just as with the Mandelbrot set, we have the following:

Proposition 2.2.6. *Any connected component W of C_N^d is simply connected.*

The next result found in [8] is a fundamental object of study in this thesis as we will analyze the sheets of the following covering.

Theorem 2.2.7. *Let W be a connected component of C_N^d with $N \geq 2$. Then, the eigenvalue map $\chi_d : W \rightarrow C_N^d$ is a $(d-1)$ -fold covering map ramified over 0.*

We next give a result which shows that as the degree d increases, the number of hyperbolic components of a given period increases.

Proposition 2.2.8. *For each $N \geq 2$, there are $\frac{d^{N-1} - 1}{d - 1}$ hyperbolic components in the interior of B_d whose period divides N .*

For example, in B_3 , there are four hyperbolic components of period 3. These components are the landing point of parameter rays of the form $\frac{j}{13}$ in Figure 2.12.

We conclude this section by showing that the hyperbolic components of B_d converge to the corresponding hyperbolic components of the exponential family.

Theorem 2.2.9. (Dynamical Convergence to the Exponential)

1. *If E_λ has an attracting periodic point of period N , then there is a D such that for $d > D$, $P_{d,\lambda}$ has an attracting periodic point of period N .*
2. *For a fixed λ , if $P_{d,\lambda}$ has an attracting periodic point of period N for infinitely many d , then E_λ has an attracting or parabolic periodic point of period N .*

2.2.2 Parameter Rays

In this section we will discuss the complement of the bifurcation diagrams B_d . In order to do this, we consider the polynomials $Q_{d,c}(z) = z^d + c$. Note that $Q_{d,c}$ is affine conjugate to $P_{d,\lambda}$, with $\lambda = dc^{d-1}$, via the conjugacy $\nu(z) = \frac{cz}{d} + c$. This means that there is a $(d - 1)$ -fold covering $\lambda = \Pi(c) = dc^{d-1}$ from the c -plane to the λ -plane. Let $\mathcal{M}_d = \{c \mid (Q_{d,c}^n)(0) \text{ is bounded for all } n\}$ be the analogue to the bifurcation diagram B_d ; these are the so-called *Multibrot sets*. Then, the map

$$\Pi|_{\mathcal{M}_d} : \mathcal{M}_d \rightarrow B_d$$

is a $(d - 1)$ -fold covering space. Following the proof in [9] for the Mandelbrot set, we can prove the following.

Proposition 2.2.10. *For each d , B_d is connected.*

Proof. We let $K_{d,c}$ denote the filled-in Julia set for $Q_{d,c}$ and we define the Green's function for $K_{d,c}$ by

$$G_{d,c}(z) = \lim_{n \rightarrow \infty} \frac{1}{d^n} \log |Q_{d,c}^n(z)|.$$

Set $U_{d,c} = \{z \mid G_{d,c}(z) > G_{d,c}(0)\}$. It is shown in [9] that there is a unique analytic mapping

$$\phi_{d,c} : U_{d,c} \rightarrow \mathbb{C}$$

which is tangent to the identity at infinity, conjugating $Q_{d,c}(z)$ to $z \mapsto z^d$. Also, see Section 2.1. Now mimic the proof in [9] to show that the mapping

$$\tilde{\Phi}_d : \mathbb{C} - \mathcal{M}_d \rightarrow \mathbb{C} - \overline{\mathbb{D}} \text{ given by } \tilde{\Phi}_d(c) = \phi_{d,c}(c)$$

is an analytic isomorphism. Hence, \mathcal{M}_d is connected for each d , and since $B_d = \Pi(\mathcal{M}_d)$, it follows that B_d is connected. \square

Following the ideas found in the previous proof, we will construct an analytic isomorphism $\Phi_d : \mathbb{C} - B_d \rightarrow \mathbb{C} - \overline{\mathbb{D}}$ that uniformizes the exterior of B_d . In analogy to the polynomials $Q_{d,c}$, we define

$$G_{d,\lambda}(z) = \lim_{n \rightarrow \infty} \frac{1}{d^n} \log |P_{d,\lambda}^n(z)| \quad \text{and} \quad U_{d,\lambda} = \{z \mid G_{d,\lambda}(z) > G_{d,\lambda}(-d)\}.$$

Recall that $\nu(z) = \frac{cz}{d} + c$ is the map conjugating $Q_{d,c}$ to $P_{d,\lambda}$. We define

$$\phi_{d,\lambda} : U_{d,\lambda} \rightarrow \mathbb{C} \quad \text{by} \quad \phi_{d,\lambda}(z) = \phi_{d,c}(\nu(z)),$$

which gives a uniformization of $U_{d,\lambda}$ conjugating $P_{d,\lambda}$ to the map $z \mapsto z^d$. Now, setting

$$\Phi_d(\lambda) = (\phi_{d,\lambda}(0))^{d-1}$$

we have the following.

Proposition 2.2.11. $\Phi_d : \mathbb{C} - B_d \rightarrow \mathbb{C} - \overline{\mathbb{D}}$ is an analytic isomorphism.

Proof. Since $\phi_{d,\lambda}(0) = \phi_{d,c}(\nu(0)) = \phi_{d,c}(c)$, we have that $\Phi_d(\lambda) = (\tilde{\Phi}_d(c))^{d-1}$. So, we get the following commutative diagram:

$$\begin{array}{ccc} \mathbb{C} - \mathcal{M}_d & \xrightarrow{\tilde{\Phi}_d} & \mathbb{C} - \overline{\mathbb{D}} \\ c \mapsto dc^{d-1} \downarrow & & \downarrow z \mapsto z^{d-1} \\ \mathbb{C} - B_d & \xrightarrow{\Phi_d} & \mathbb{C} - \overline{\mathbb{D}} \end{array}$$

Since $\tilde{\Phi}_d$ is an isomorphism, we have our result. \square

The most significant rays are those of rational angle θ , as these rays are known to land on the boundaries of the various B_d . In fact, these rays are used in further understanding the structure of B_d . In fact, we have the following structure theorem.

Definition 2.2.12. (Essential Parameters)

A parabolic parameter is called essential (respectively, non-essential) if the associated orbit portrait is essential (respectively, non-essential).

Definition 2.2.13. (Roots and Co-Roots)

Let W be hyperbolic component of B_d of period N . A parameter on ∂W with an essential parabolic orbit of ray period N is called a root of W . A parameter on ∂W with a non-essential parabolic orbit of ray period N is called a co-root of W .

Theorem 2.2.14. The parameter plane B_d , along with its parameter rays satisfy the following:

- (1) *Every periodic parameter ray lands at a parabolic parameter of B_d .*
- (2) *Every non-essential parabolic parameter in B_d is the landing point for exactly one periodic parameter ray.*
- (3) *Every essential parabolic parameter in B_d is the landing point for exactly two periodic parameter rays.*
- (4) *Every preperiodic parameter ray lands at a Misiurewicz point.*
- (5) *Every Misiurewicz point is the landing point of at least one preperiodic parameter ray.*
- (6) *Every hyperbolic component of B_d has exactly one root and $d - 2$ co-roots.*

[Note: Parts (4) and (5) of the above theorem will not be used in this thesis, but are included for completeness.]

Proof. The proof of this theorem really goes back to ideas that can be traced through Douady-Hubbard, Milnor, and many others. For a complete proof in the case of the parameter plane \mathcal{M}_d , see [12]. The results there then carry over to our parameter plane via the holomorphic covering map $\mathcal{M}_d \rightarrow B_d$ defined earlier. \square

Taken together, the results of this section leads to the pictures of parameter rays to B_3 and B_4 shown in Figures 2.12 and 2.13.

2.2.3 Size of B_d .

For each $d \geq 2$, the connectivity locus B_d is a compact subset of the plane, but the diameter of these sets grows as d increases. This is in contrast to the Multibrot sets

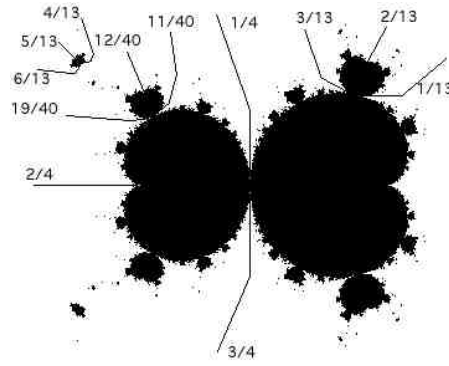


Figure 2.12: The bifurcation diagram B_3 and some parameter rays.

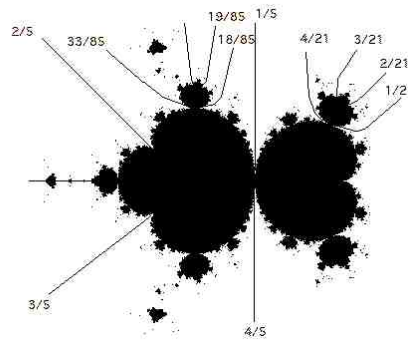


Figure 2.13: The bifurcation diagram B_4 and some parameter rays.

\mathcal{M}_d , which for each d , are contained in the closed disc of radius 2 about the origin. The growth of B_d is, however, consistent with the fact that the B_d converge to the bifurcation diagram for $z \mapsto \lambda e^z$, which is unbounded. In this section, we show that for a fixed d we can estimate the size of B_d which will be useful later when we prove the convergence of the modified Spider Algorithm .

First, we have the following sharper result about the size of the Multibrot sets \mathcal{M}_d .

Proposition 2.2.15. \mathcal{M}_d is contained in $\overline{D}\left(0, 2^{\frac{1}{d-1}}\right)$, the closed disc about the

origin of radius $2^{\frac{1}{d-1}}$.

Remark 2.2.16. Note that this result shows that the Multibrot sets actually decrease in size as d increases, being contained in discs that approach the closed unit disc.

Proof. Note that

$$|c| > 2^{\frac{1}{d-1}} \implies |Q_{d,c}(c)| = |c^d + c| \geq |c|^d - |c| = |c|(|c|^{d-1} - 1) > 2^{\frac{1}{d-1}}.$$

Then, by induction, we have $|Q_{d,c}^n(c)| > 2^{\frac{n}{d-1}}$ for all $n \geq 1$. \square

Corollary 2.2.17. $B_d \subset \overline{D}(0, 2d)$.

Proof. Recall that the covering map $\mathcal{M}_d \rightarrow B_d$ is given by $c \mapsto \lambda = dc^{d-1}$. So,

$$\lambda \in B_d \implies c \in \mathcal{M}_d \implies |\lambda| = d|c|^{d-1} \leq d \left(2^{\frac{1}{d-1}}\right)^{d-1} = 2d.$$

\square

We also have a similar result for the filled-in Julia sets $K_{Q_{d,c}}$.

Corollary 2.2.18. If $c \in \mathcal{M}_d$, then $K_{Q_{d,c}} \subset \overline{D}\left(0, 2^{\frac{1}{d-1}}\right)$.

Proof. If $|z| > 2^{\frac{1}{d-1}}$, then $|z| > (2 + \epsilon)^{\frac{1}{d-1}}$ for some $\epsilon > 0$. By Proposition 2.2.15, $|c| < 2^{\frac{1}{d-1}} < |z|$. So,

$$\begin{aligned} |Q_{d,c}(z)| &\geq |z|^d - |c| > |z|^d - |z| \\ &= |z|(|z|^{d-1} - 1) \\ &> |z| \left[\left((2 + \epsilon)^{\frac{1}{d-1}} \right)^{d-1} - 1 \right] \\ &= (1 + \epsilon)|z|. \end{aligned}$$

Then, by induction, $|Q_{d,c}^n(z)| > (1 + \epsilon)^n |z|$, which converges uniformly to infinity. \square

It is not true that the filled-in Julia sets $K_{P_{d,\lambda}}$ for $\lambda \in B_d$ are bounded. In fact, $0 \in B_d$ and $K_{P_{d,0}} = \mathbb{C}$. However, if $\lambda \in B_d$ is bounded away from 0, then $K_{P_{d,\lambda}}$ is bounded.

Proposition 2.2.19. *Fix $\epsilon > 0$. If $\lambda \in B_d$ and $|\lambda| > \epsilon$, then $K_{P_{d,\lambda}}$ is contained in the disc centered at $-d$ with radius $d \left(\frac{2d}{\epsilon}\right)^{\frac{1}{d-1}}$.*

Proof. If $|z + d| > d \left(\frac{2d}{\epsilon}\right)^{\frac{1}{d-1}}$, then $|z + d| > (1 + \delta)d$ for some $\delta > 0$, since $\epsilon < 2d$. So,

$$\begin{aligned} |P_{d,\lambda}(z)| &= \frac{|\lambda|}{d^d} |z + d|^d > \frac{\epsilon}{d^d} |z + d|^d \\ &= \frac{\epsilon}{d^d} |z + d|^{d-1} |z + d| \\ &> \frac{\epsilon}{d^d} d^{d-1} \left(\frac{2d}{\epsilon}\right) |z + d| \\ &= 2|z + d| \\ &> 2(1 + \delta)d. \end{aligned}$$

Next,

$$\begin{aligned} |P_{d,\lambda}(z) + d| &> |P_{d,\lambda}(z)| - d \\ &> 2|z + d| - d \\ &> |z + d| + (1 + \delta)d - d \\ &= |z + d| + \delta d. \end{aligned}$$

Then,

$$\begin{aligned}
 |P_{d,\lambda}^2(z)| &= \frac{|\lambda|}{d} |P_{d,\lambda}(z) + d|^d > \frac{\epsilon}{d^d} |P_{d,\lambda}(z) + d|^{d-1} |P_{d,\lambda}(z)z + d| \\
 &> \frac{\epsilon}{d^d} d^{d-1} \left(\frac{2d}{\epsilon} \right) (|z + d| + \delta d) \\
 &= 2|z + d| + 2\delta d.
 \end{aligned}$$

Continuing inductively, we find that $|P_{d,\lambda}^n(z)| > 2|z + d| + 2n\delta d$. □

Chapter 3

Analytic Preliminaries

3.1 Introduction

In this chapter, we gather together some of the analytic notions that will be used throughout the thesis, including some basic theory of Teichmüller spaces, quadratic differentials, and univalent mappings.

Definition 3.1.1. (Univalent Function)

If U is an open subset of $\hat{\mathbb{C}}$, we say that $f : U \rightarrow \hat{\mathbb{C}}$ is univalent if f is analytic and injective on U . Note that U need not be connected.

3.2 Quadratic Differentials

In this section, we discuss spaces of quadratic differentials on Riemann surfaces. As we will see later, the complex analytic structure of Teichmüller space is intimately related to holomorphic quadratic differential forms. Let X be a Riemann surface.

Definition 3.2.1. (Quadratic Differentials)

A quadratic differential q on X is $(2, 0)$ -tensor given locally by $q = q(z)dz^2$. We say that q is holomorphic if $q(z)$ is holomorphic.

Remark 3.2.2. Another way to define a quadratic differential is to note that it is a section of the square of the canonical bundle on the Riemann surface X .

If $q(x) \neq 0$, then there is a local chart w near x for which $q = dz^2$. This chart is unique up to translation and sign and it is given locally by

$$w(y) = \int_x^y \sqrt{q}.$$

Note here that \sqrt{q} is a holomorphic 1-form. If $q(x) = 0$, then there is a local chart in which $q = z^n dz^2$, for some $n > 0$.

A quadratic differential determines a metric $|q|$ on X since locally, $|q(z)dz^2| = |q(z)|dx dy$. We say that a quadratic differential is *integrable* if

$$\|q\| := \int_X |q| < \infty. \quad (3.1)$$

Let $Q(X)$ denote the Banach space of integrable quadratic differentials on X with the L^1 -norm above. The norm of q is simply the total area of q on X with respect to the metric $|q|$.

Theorem 3.2.3. *Let X be a Riemann surface of finite type; that is, X is obtained from a compact Riemann surface by puncturing at a finite number of points. Then $Q(X)$ consists of the holomorphic quadratic differentials on X which have, at worst, simple poles at the punctures of X .*

Another norm on quadratic differentials is the *hyperbolic sup-norm*. Let X be a hyperbolic Riemann surface with its hyperbolic metric ρ . Define

$$\|q\|_\infty = \sup_{x \in X} \frac{|q(x)|}{\rho(x)^2} \quad (3.2)$$

Since $|q|/\rho^2$ is a function on X , we are justified in taking a supremum. The norm defined by (3.2) is called the *hyperbolic sup-norm* of q .

Let $B(X)$ denote the Banach space of holomorphic quadratic differentials on X for which the hyperbolic sup-norm is bounded.

3.3 Schwarzian Derivative

There is a very useful relationship between univalent functions and quadratic differentials via the Schwarzian derivative. If f is univalent on some domain D , then the *Schwarzian derivative* of f is defined by

$$S\{f\} = \left(\frac{f''}{f'}\right)' - \frac{1}{2} \left(\frac{f''}{f'}\right)^2$$

Since f is univalent, $f' \neq 0$, and so $S\{f\}$ is well-defined. The definition of the Schwarzian derivative is not nearly as important as its properties.

Proposition 3.3.1. *Let f and g be univalent in a domain D . Then,*

$$(i) \quad S\{f\} = 0 \iff f \text{ is a Möbius transformation.}$$

$$(ii) \quad S\{f \circ g\} = (S\{f\} \circ g)(g')^2 + S\{g\}.$$

Proof. Straightforward computation. □

Remarks 3.3.2. *The first part of this proposition can be interpreted as a geometric result which indicates that the Schwarzian derivative measures how far a univalent function deviates from being a Möbius transformation. Also, note that $S\{f \circ g\} = S\{g\}$ if f is a Möbius transformation. Thus, the Schwarzian derivative of a univalent function is invariant under post-composition by Möbius transformations.*

A very important observation related to part (ii) of Proposition 3.3.1 is that the Schwarzian derivative has the transformation property of quadratic differentials. That is, if f is univalent and g is a Möbius transformation, then

$$S\{f \circ g\} = (S\{f\} \circ g)(g')^2.$$

Thus, we can identify the image of a univalent function under the Schwarzian derivative as a quadratic differential.

Since the interplay between univalent mappings and Schwarzian derivatives plays an important role in this thesis, we gather together some of the basic results about Schwarzian derivatives in a series of propositions.

Let D be any domain which is Möbius equivalent to the unit disc and let $\rho(z)|dz|$ be the hyperbolic metric on D . Let f be univalent in D and assign the hyperbolic sup-norm to $S\{f\}$:

$$\|S\{f\}\|_D = \sup_{z \in D} |S\{f\}|\rho(z)^{-2}.$$

Proposition 3.3.3. *If f is univalent in D , then $\|S\{f\}\|_D \leq \frac{3}{2}$.*

Proof. This fact follows easily from the Area Theorem. See [17] □

Thus, univalent functions have finite hyperbolic sup-norm.

Proposition 3.3.4. *Suppose that g is univalent in a disc A and that f is meromorphic and locally one-to-one in A . Then,*

$$\|S\{f\} - S\{g\}\|_A = \|S\{f \circ g^{-1}\}\|_{g(A)}. \quad (3.3)$$

Proof. Let $\rho_A|dz|$ denote the hyperbolic metric on A and similarly for $\rho_B|dz|$, where $g(A) = B$.

$$\begin{aligned} \|S\{f\} - S\{g\}\|_A &= \sup_{z \in A} \frac{|S\{f\}(z) - S\{g\}(z)|}{(\rho_A(z))^2} \\ &= \sup_{w \in B} \frac{|S\{f\}(g^{-1}(w)) - S\{g\}(g^{-1}(w))|}{(\rho_B(w)|(g^{-1})'(w)|)^2} \\ &= \sup_{w \in B} \frac{|S\{f \circ g^{-1}\}(w) - S\{g \circ g^{-1}\}(w)|| (g^{-1})'(w)|^2}{(\rho_B(w)|(g^{-1})'(w)|)^2} \\ &= \|S\{f \circ g^{-1}\}\|_{g(A)}. \end{aligned}$$

□

The next two results tell us that we can solve the Schwarzian differential equation and that, under certain circumstances, the solution is univalent.

Proposition 3.3.5. *Let q be any holomorphic quadratic differential on a simply connected domain $D \subset \mathbb{C}$. Then, there exists a function f , meromorphic in D , such that $S\{f\} = q$. The solution is unique up to post-composition by a Möbius transformation.*

Proof. Consider the *hypergeometric differential equation*

$$w'' + \frac{q}{2}w = 0, \quad (3.4)$$

which is a linear differential equation. Hence, (3.4) has linearly independent holomorphic solutions in D , say w_1 and w_2 . Since there is no w' term in (3.4), the Wronskian $w_1w_2' - w_2w_1'$ is constant, which we normalize to be 1. Then, setting $f = \frac{w_1}{w_2}$, we have

$$f' = \frac{w_2w_1' - w_1w_2'}{w_2^2} = \frac{-1}{w_2^2}$$

and

$$f'' = \frac{2w_2'}{w_2^3}.$$

Hence,

$$\begin{aligned} S\{f\} &= \left(\frac{f''}{f'}\right)' - \frac{1}{2} \left(\frac{f''}{f'}\right)^2 \\ &= \left(\frac{-2w_2'}{w_2}\right)' - \frac{1}{2} \left(\frac{-2w_2'}{w_2}\right)^2 \\ &= \frac{-2w_2w_2'' + 2(w_2')^2}{w_2^2} - \frac{1}{2} \left(\frac{4(w_2')^2}{w_2^2}\right) \\ &= -2\frac{w_2''}{w_2} \\ &= q \quad \text{by (3.4).} \end{aligned}$$

□

We now have the following extension theorem. A *quasidisc* is the image of the unit disc under a quasiconformal mapping.

Proposition 3.3.6. *Let D be a quasidisc. Then, there is a constant $\epsilon > 0$ such that if f is meromorphic in D and $\|S\{f\}\| < \epsilon$, then f is univalent in D and has a quasiconformal extension to $\hat{\mathbb{C}}$.*

3.4 Teichmüller Theory

3.4.1 Quasiconformal Mappings

Definition 3.4.1. (Quasiconformal mappings)

Let X and Y be hyperbolic Riemann surfaces. A mapping $f : X \rightarrow Y$ is called K -quasiconformal ($K \geq 1$) if it is an orientation-preserving homeomorphism, it has distributional derivatives

$$f_z = \frac{\partial f}{\partial z}, \quad f_{\bar{z}} = \frac{\partial f}{\partial \bar{z}}$$

which are locally in L^2 , and the complex dilatation μ_f given locally by

$$\mu_f(z) \frac{d\bar{z}}{dz} = \frac{f_z d\bar{z}}{f_{\bar{z}} dz}$$

satisfies $|\mu_f| \leq \frac{K-1}{K+1}$ almost everywhere.

The definition of quasiconformality implies that f_z is non-zero almost everywhere, and therefore, μ_f is a well-defined object. In fact, μ_f is called a *Beltrami differential*; that is, μ_f is a differential form of type $(-1,1)$.

A quasiconformal mapping, f , of $\hat{\mathbb{C}}$ is called *normalized* if f fixes the points $0, 1, \infty$.

A fundamental result related to quasiconformal mappings is the fact any μ with $\|\mu\|_\infty < 1$ gives rise to a quasiconformal map. This result is called the **Measurable Riemann Mapping Theorem**.

Theorem 3.4.2. (Ahlfors-Bers)

For any L^∞ Beltrami form μ on $\hat{\mathbb{C}}$ with $\|\mu\|_\infty < 1$, there is a unique normalized quasiconformal mapping $w^\mu : \hat{\mathbb{C}} \rightarrow \hat{\mathbb{C}}$ such that the complex dilatation of w^μ is μ .

Furthermore, for any μ with $\|\mu\|_\infty < 1$, there is a family of normalized quasiconformal mappings $w_t^\mu : \hat{\mathbb{C}} \rightarrow \hat{\mathbb{C}}$, $|t| < 1$, satisfying

$$\frac{(w_t^\mu)_{\bar{z}}}{(w_t^\mu)_z} = t\mu.$$

Then, $w_t^\mu(z)$ is a holomorphic function of t (t in the unit disc) for each $z \in \hat{\mathbb{C}}$.

3.4.2 Classical Teichmüller Space

We begin with the classical construction of Teichmüller space. Let X be a Riemann surface of finite type; i.e., $X = \bar{X} - E$, where \bar{X} is compact and E is some finite set. We define the Teichmüller space of X , denoted $\text{Teich}(X)$, to be the set of pairs (Y, ϕ) where Y is a Riemann surface and $\phi : X \rightarrow Y$ is a quasiconformal mapping, modulo the following equivalence relation. Two pairs (Y_1, ϕ_1) and (Y_2, ϕ_2) are equivalent if there exists a conformal isomorphism $\alpha : Y_1 \rightarrow Y_2$ such that $\phi_2 = \alpha \circ \phi_1$ on E and ϕ_2 is isotopic to $\alpha \circ \phi_1$ rel E .

Note $\text{Teich}(X)$ is a metric space with the metric:

$$d((Y_1, \phi_1), (Y_2, \phi_2)) = \inf_f \log K(f),$$

where the infimum is taken over all quasiconformal mappings f such that $\phi_2 = f \circ \phi_1$ on E and ϕ_2 is isotopic to $f \circ \phi_1$ rel E .

There is an alternate description of Teichmüller space coming from the Ahlfors-Bers Theorem (Theorem 3.4.2). Let $M(X)$ denote the open unit ball of the complex

Banach space $L^\infty(X)$. Then, there is a natural map

$$\Phi : M(X) \rightarrow \text{Teich}(X) \quad \text{given by} \quad \Phi(\mu) = [w^\mu] \quad (3.5)$$

where $[w^\mu]$ is the equivalence class (in the sense given above) of the unique normalized quasiconformal map w^μ which has Beltrami coefficient μ .

Combining results from the previous sections, we arrive at the following result.

Theorem 3.4.3. *There exists a unique complex analytic manifold structure on $\text{Teich}(X)$ such that $\Phi : M(X) \rightarrow \text{Teich}(X)$ is a holomorphic split submersion.*

Remark 3.4.4. *The idea behind the proof of this theorem is due to Bers and relies on the fact that $\text{Teich}(X)$ can be embedded in a space of quadratic differentials on the conjugate Riemann surface, X^* .*

Proof. (sketch)

We assume that X is a hyperbolic Riemann surface and let $\pi : \mathbb{H} \rightarrow X$ be a universal covering map with covering group G . Then, $\pi^* : M(X) \rightarrow M(\mathbb{H})$ maps the Beltrami forms on X isomorphically onto the G -invariant Beltrami forms on \mathbb{H} . This is the space $M_G(\mathbb{H}) = \{\mu \in M(\mathbb{H}) : (\mu \circ g)(\overline{g'}/g') = \mu, \text{ for all } g \in G\}$.

Extend each $\pi^*\mu$ to $\hat{\mathbb{C}}$ as follows and denote this extension by $\tilde{\mu}$.

$$\tilde{\mu} = \begin{cases} \pi^*\mu & \text{in } \mathbb{H} \\ 0 & \text{in } \overline{\mathbb{H}} \end{cases}$$

Then, Theorem 3.4.2 gives a quasiconformal mapping $w^{\tilde{\mu}} : \hat{\mathbb{C}} \rightarrow \hat{\mathbb{C}}$ which is *univalent* in the lower half-plane, $\overline{\mathbb{H}}$. Hence, we can apply the Schwarzian derivative to $w^{\tilde{\mu}}$ in the lower half-plane.

Define $\mathcal{P} : M_G(\mathbb{H}) \rightarrow B_G(\overline{\mathbb{H}})$ by

$$\mathcal{P}(\mu) = S\{w^{\tilde{\mu}}|_{\overline{\mathbb{H}}}\}. \quad (3.6)$$

Here, $B_G(\overline{\mathbb{H}})$ is the space of G -invariant holomorphic quadratic differentials on the lower half-plane. Since $B_G(\overline{\mathbb{H}})$ is isometrically isomorphic to $B(X^*)$, we get a mapping from $M(X)$ into $B(X^*)$, which descends to a map $\mathcal{B} : \text{Teich}(X) \rightarrow B(X^*)$. This map is called the *Bers embedding* of Teichmüller space.

By Proposition 3.3.3, $U = \mathcal{B}(\text{Teich}(X))$ is a bounded subset of $B(X^*)$. Furthermore, using Proposition 3.3.6 we can show that U is open and that there is a real-analytic section $s : U \rightarrow \text{Teich}(X)$. \square

3.5 Holomorphic Motions

Holomorphic motions are very useful in the study of complex dynamical systems and of Teichmüller spaces.

Definition 3.5.1. *Let V be a connected complex manifold with basepoint λ_0 and let X be a subset of $\hat{\mathbb{C}}$. A holomorphic motion of X over V is a map $\phi : V \times X \rightarrow \hat{\mathbb{C}}$ such that*

- (a) $\phi(\lambda_0, x) = x$ for all $x \in X$,
- (b) for each $x \in X$, the map $t \mapsto \phi(\lambda, x)$ is analytic, and
- (c) for each $\lambda \in V$, the map $x \mapsto \phi(\lambda, x)$ is injective.

Example 3.5.2. *Let $M(\mathbb{C})$ be the open unit ball in $L^\infty(\mathbb{C})$. Define $\phi : M(\mathbb{C}) \times \hat{\mathbb{C}} \rightarrow \hat{\mathbb{C}}$ by*

$$\phi(\mu, z) = w^\mu(z),$$

where w^μ is the unique normalized quasiconformal mapping of $\hat{\mathbb{C}}$ with complex dilatation μ . By Theorem 3.4.2, ϕ is a holomorphic motion of $\hat{\mathbb{C}}$ over $M(\mathbb{C})$.

A basic result about holomorphic motions is the following result of Mañé, Sad, and Sullivan (see [24]).

Theorem 3.5.3. (The λ -Lemma)

A holomorphic motion of X has a unique extension to a holomorphic motion of \overline{X} . The extended holomorphic motion is a continuous map $\phi : V \times \overline{X} \rightarrow \hat{\mathbb{C}}$. For each λ , the map $\phi_\lambda : X \rightarrow \hat{\mathbb{C}}$ extends to a quasiconformal map of the sphere to itself.

This result is used in proving the following result about extending holomorphic motions. For a proof, see [14].

Theorem 3.5.4. (Slodkowski's Theorem)

Suppose that $V = \mathbb{D}$. Then, any holomorphic motion $\phi : V \times X \rightarrow \hat{\mathbb{C}}$ extends to a holomorphic motion $\tilde{\phi} : V \times \hat{\mathbb{C}} \rightarrow \hat{\mathbb{C}}$. Furthermore, for each $\lambda \in V$, the maps $\tilde{\phi}_\lambda$ are quasiconformal mappings of the sphere.

Remark 3.5.5. *Actually, this theorem is true for V any simply-connected Riemann surface.*

Chapter 4

Spider Space and the Spider Map

In this chapter, we introduce the two primary players in this thesis: Spider Space, which is built of combinatorial and analytic data, and Spider mappings, which are holomorphic self-mappings of Spider Space. There are infinitely many Spider mappings on Spider Space and we characterize all of these mappings in Section 4. The iteration of Spider mappings leads to fixed points in Spider Space, and this is proved in Chapter 6. In Section 5 of this chapter, we show that the existence of such fixed points provides an answer to Question 1 posed in Chapter 1.

The data given is a choice of external angle θ , a multiplier μ with $0 < |\mu| < 1$ and a degree d . The combinatorics of the external ray of angle θ allows us to pick appropriate branches of $P_{\lambda,d}^{-1}$ in determining the correct polynomial. We will see that different choices of branches leads to different polynomials and that after adding $2\pi(d-1)$ to the argument of any branch, we return to the same polynomial. The key to this algorithm is identifying the correct logarithms, which is encoded in a kneading sequence and in the winding of curves described below.

4.1 Standard Clubbed Spider

Given the data d , θ , and μ , as specified in Question 1, we construct the following combinatorial object called the *Standard Spider*:

$$S_{\theta,\mu} = \bigcup_{j=1}^N L_j \cup \bigcup_{j=1}^N \overline{D}_j \cup \{\infty\},$$

where the open discs $D_j \subset \{z : |z| < 1\}$ are discs are constructed so that

$$\overline{D}_j \cap \{z : |z| = 1\} = e^{2\pi i d^{j-1} \theta} \quad \text{and} \quad \overline{D}_i \cap \overline{D}_j = \emptyset, \text{ for } i \neq j.$$

These discs form the feet of our standard spider and its legs are the rays

$$L_j = \{r e^{2\pi i d^{j-1} \theta} \mid r \geq 1\}$$

where $j = 1, \dots, N$.

Next, we specify a sequence of distinguished points in each foot, converging geometrically to the center of the foot. For each $j = 1, \dots, N$, this is the set of points $\{x_{j+kN} = \mu^k(x_j - c_j) + c_j \mid k = 1, 2, 3, \dots\}$, where c_j is the center of D_j .

Figure 4.1 displays a standard spider picture; the extra information in the picture will be explained in the following sections.

4.1.1 The Looping Number

As stated in the introduction to this chapter, we need to differentiate between different branches of $P_{\lambda,d}^{-1}$; this date is encoded in the wrapping of paths around the feet of the spiders to follow. We specify a path, Γ , connecting x_1 to x_{1+N} inside the first foot; see Figure 4.1. The convergence of the spider algorithm to the desired

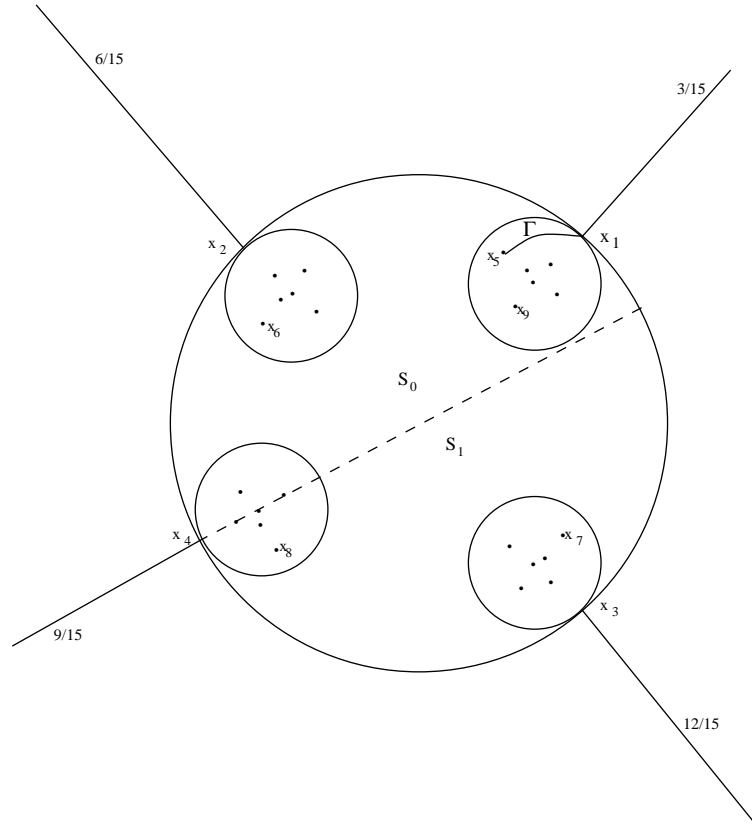


Figure 4.1: Standard spider for $\theta = \frac{3}{15}$, $\mu = 0.5i$, $d = 2$

polynomial depends on the homotopy type of this path. Note that x_{1+N} is separated from x_1 by the annulus

$$\mathcal{A} = \{z : |\mu|R < |z - c_1| < R\},$$

where c_1 is the center of D_1 and R is the radius of D_1 . Also note that \mathcal{A} does not contain any of the distinguished points in D_1 , but x_1 and x_{1+N} lie on the outer and inner boundaries of \mathcal{A} , respectively. Let Γ be any continuous path from x_1 to x_{1+N} that travels only through \mathcal{A} and does not cross itself. Since we are interested in the homotopy type of this path (i.e., number of windings around the compact

component of $\mathbb{C} - \mathcal{A}$), we only consider paths that travel exclusively clockwise or counter-clockwise.

Let $\alpha(\Gamma)$ be the number of radians through which Γ turns about the center c_1 , with the convention that $\alpha(\Gamma)$ is positive if Γ travels counter-clockwise from x_1 and is negative if Γ travels clockwise. So, taking $\arg(\mu) \in [0, 2\pi)$, we have

$$\alpha(\Gamma) = \begin{cases} 2\pi\ell + \arg(\mu) & \text{if } \Gamma \text{ travels counter-clockwise} \\ 2\pi\ell + (\arg(\mu) - 2\pi) & \text{if } \Gamma \text{ travels clockwise.} \end{cases}$$

Definition 4.1.1. *The number, ℓ , which is an integer, captures the number of complete loops (and the direction of looping) Γ makes before terminating at x_{1+N} . We call this number the Looping Number for Γ .*

Figure 4.2 displays some looping numbers.

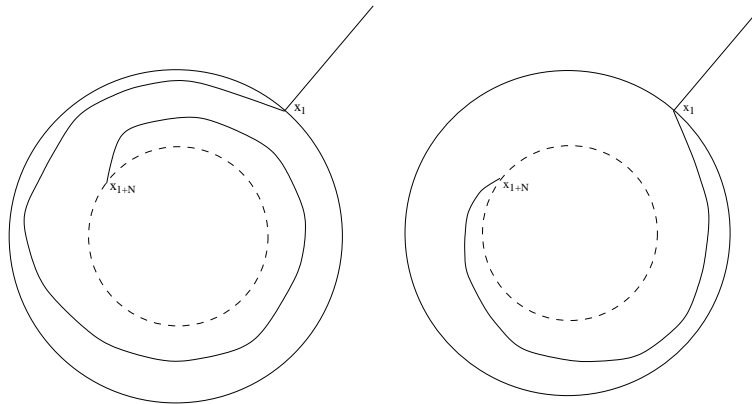


Figure 4.2: Looping numbers. The left picture has $\alpha(\Gamma) = +\frac{5\pi}{2}$ and $\ell = +1$. The right picture has $\alpha(\Gamma) = -\frac{3\pi}{2}$ and $\ell = 0$.

4.1.2 A Kneading Sequence

Since our algorithm involves choosing a particular inverse branch of an analytic map, we require a method of identifying the correct branch; the data for this choice comes from a kneading sequence. On the standard spider picture, separate the closed unit disc into d sectors by drawing the radii connecting 0 to $e^{2\pi i \frac{\theta}{d}}, e^{2\pi i \frac{\theta+1}{d}}, \dots, e^{2\pi i \frac{\theta+d-1}{d}}$; these points on the unit circle are the d preimages of x_1 under $t \mapsto dt$. Label the sector containing x_1 with S_0 and then label the remaining sectors, in counter-clockwise direction, with S_1, \dots, S_{d-1} . Then, for $j = 1, \dots, N - 1$, we set:

$$knead(j) = S_n \quad \text{if } x_j \text{ is in } S_n.$$

Now, since θ is periodic, the point x_N will be one of the d points: $e^{2\pi i \frac{\theta}{d}}, \dots, e^{2\pi i \frac{\theta+d-1}{d}}$ and its label can be determined by where x_N lies in the circular order as we travel counter-clockwise around the unit circle. If, as we travel, we pass from S_m into S_n at x_N then set $knead(N) = S_n^m$, where the indices m and n are to be taken mod d . The standard spider along with the sector sequence and the looping number provides all the information needed to find the specified polynomial. For example, the sector(kneading) sequence associated with $\theta = \frac{3}{15}$ and $d = 2$ is $S_0 S_0 S_1 S_1^0$.

4.2 Spider Space

We are now ready to define the Spider space, $\mathcal{T}_{\theta,\mu}$. We begin with

Definition 4.2.1. (Spiders)

A spider $\varphi : S_{\theta,\mu} \rightarrow \hat{\mathbb{C}}$ is a mapping defined on the Standard Spider which satisfies:

- (1) φ is a continuous and injective,
- (2) φ is univalent on $\cup D_j$,
- (3) $\varphi(x_1) = 0$ and $\varphi(\infty) = \infty$ and
- (4) φ respects circular order at infinity.

Note that the third condition in the above definition is a statement about the legs of the spider. It says that φ preserves the order in which the legs of the Standard Spider approach infinity.

We denote the set of all spiders by $\mathcal{T}_{\theta,\mu}^0$ and define *Spider Space* as the quotient

$$\mathcal{T}_{\theta,\mu} = \mathcal{T}_{\theta,\mu}^0 / \sim$$

where $\varphi_1 \sim \varphi_2$ if φ_1 is isotopic to φ_2 rel $\varphi_1(\cup \overline{D}_j)$.

We refer to $\cup \varphi(\overline{D}_j)$ as the *feet* of the spider φ . Note that, since the spiders are required to be continuous on $\cup \partial D_j$ and fix infinity, the feet of the spider are compact subsets of \mathbb{C} .

We think of two spiders being equivalent if we can continuously deform the legs of one onto the legs of the other, while keeping the feet stationary. Figure 4.3 shows some typical spiders; the top two belong to the same equivalence class, while the bottom one is not equivalent to the other two.

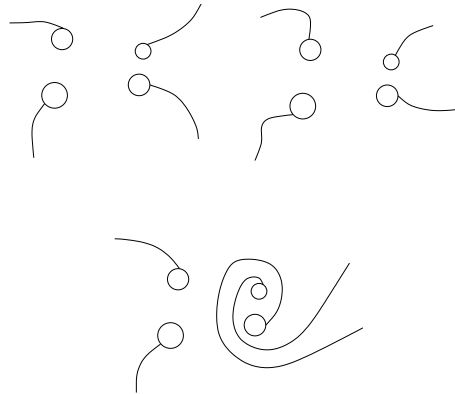


Figure 4.3: Some typical spiders for a period 4 cycle.

4.3 Spider Mappings

Let ℓ be the looping number for Γ in the standard spider and define a mapping $\sigma_\ell : \mathcal{T}_{\theta, \mu} \rightarrow \mathcal{T}_{\theta, \mu}$ as follows. Given a representative, φ , from $[\varphi] \in \mathcal{T}_{\theta, \mu}$, we will produce a new spider, $\tilde{\varphi}$, such that $\sigma_\ell([\varphi]) = [\tilde{\varphi}]$. Consider the polynomial $P(z) := P_{\varphi(x_2)}(z) = \varphi(x_2)(1 + \frac{z}{d})^d$ and use the kneading sequence associated with θ to choose a branch of P^{-1} . Since the leg $\varphi(L_1)$ leads to the critical value 0 of P , we see that $P^{-1}(\varphi(L_1))$ consists of d curves meeting at $-d$ and dividing the complex plane into d sectors; label the sector containing 0 with S_0 and label the others sequentially in a counter-clockwise fashion with S_1, \dots, S_{d-1} .

For $j = 1, \dots, N - 1$, let $\tilde{\varphi}(x_j)$ be the point in $P^{-1}(\varphi(x_{j+1}))$, which lies in the sector given by $knead(j)$. Next, define $\tilde{\varphi}(L_j)$ to be the curve in $P^{-1}(\varphi(L_{j+1}))$ leading to $\tilde{\varphi}(x_j)$ and let $\tilde{\varphi}(D_j)$ be the preimage of $\varphi(D_{j+1})$ which has $\tilde{\varphi}(x_j)$ on its boundary. Thus, we have now specified all but one of the legs and feet of a new spider.

4.3.1 Defining the Final Leg and Final Foot

We now define the method for determining in which sector $(S_0, S_1, \dots, S_{d-1})$ the final foot of the spider should be defined. In what we have done up to this point, we have used combinatorial data related to the input angle θ to determine our spider map; we need only add a little more combinatorics to finish the description. A slight modification we use is that we now assume that $\theta_1 = \theta$ and that $\theta_1 < \theta_2$, where θ_2 is the angle of the companion ray that lands with the ray of angle θ at the principal root of the hyperbolic component determined by θ . This modification is justified since either of the two rays landing at the principal root will determine the same polynomial.

Recall that the last entry in the kneading sequence for θ_1 is of the form S_{i+1}^i , where the indices are to be taken modulo d . This means that $d^{N-1}\theta_1$ is the ray separating sector S_i from S_{i+1} and $d^{N-1}\theta_1$ is the unique periodic (of period N) pre-angle of θ_1 . We now add the orbit of θ_2 to our standard spider picture and consider the orbit portrait of the polynomials in the hyperbolic component. The orbit portrait is obtained by indicating the orbits of both θ_1 and θ_2 on \mathbb{S}^1 and connecting (inside the circle) the rays that land together in the Julia set. In the Julia set, these rays land on the repelling orbit of the principal root of the Fatou components containing the attracting cycle. In other words, we will analyze the data coming from a known Julia set of a polynomial in our hyperbolic component combined with the spider information in order to determine which is the preferred sector for the final foot.

Note that $\mathcal{R}_{d^{N-1}\theta_2}$ is the ray in the Julia set that lands with $\mathcal{R}_{d^{N-1}\theta_1}$ at the principal root of the Fatou component containing the critical point. Since $d^{N-1}\theta_2$ is

periodic of period N , it cannot land at the boundary of any of the sectors determined by θ_1 . This follows from the fact that θ_1 has only one pre-image under the d -tupling map which is periodic. Hence, $d^{N-1}\theta_2$ lies strictly inside one of the sectors, and so, the principal repelling root at which both $d^{N-1}\theta_1$ and $d^{N-1}\theta_2$ land is also in this sector. Since the attracting periodic point in the Fatou component containing the critical value lies in the same sector as this principal repelling root, we will have determined the correct sector once we identify the sector in which $d^{N-1}\theta_2$ lies.

Figure 4.4 illustrates the procedure explained here. For $d = 3$, we have shown the orbit portrait for the rays corresponding to the angles $\theta_1 = \frac{4}{80}$ and $\theta_2 = \frac{6}{80}$ and we note that these rays land at the principal root of a period 4 hyperbolic component in the degree 3 parameter space. The heavy black dots represent the principal repelling roots of the Fatou components containing the attracting periodic cycle.

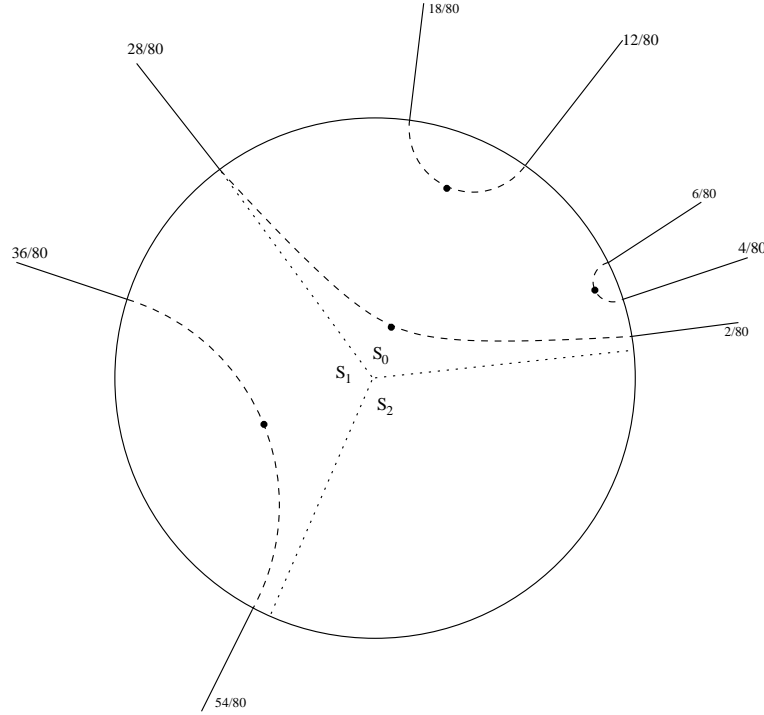


Figure 4.4: The orbit portrait for $\theta = \frac{4}{80}$ and $d = 3$.

Proposition 4.3.1. *If the last entry of $\text{knead}(\theta_1) = S_{i+1}^i$, then the dynamic ray of external angle $d^{N-1}\theta_2$ lies in sector S_i .*

Proof. The orbit portrait for polynomials associated with the angle θ_1 , contains the angles

$$\theta_1, \theta_2, d\theta_1, d\theta_2, \dots, d^{N-1}\theta_1, d^{N-1}\theta_2$$

with repetitions possible in this list if the orbit portrait is not primitive. The complementary arc $(d^{N-1}\theta_1, d^{N-1}\theta_2)$ is the critical arc in that it covers the arc (θ_1, θ_2) exactly d times. Hence, by Lemma 2.1.18, this arc has circular length greater than $1 - 1/d$. Since $d^{N-1}\theta_1$ lies on the separator of sectors S_i and S_{i+1} , and each sector has length $1/d$, it follows that $d^{N-1}\theta_2$ lies in sector S_i . \square

Thus, we see that the kneading sequence of θ_1 is all that we need in order to determine which is the preferred sector; namely, you always take an immediate left (when travelling from infinity) from the leg of the spider that goes through the critical point. The preimage, Ω , of $\varphi(D_1)$ in this sector will contain our final foot.

So, we now have a curve terminating at $-d$ along with a “foot” attached, but this is not the N^{th} foot and leg since $\tilde{\varphi}(x_N) \neq -d$. Notice that $\varphi(x_{1+N})$ is in the interior of $\varphi(D_1)$ and hence $\tilde{\varphi}(x_N)$ is in the interior of Ω . We require that the N^{th} foot has $\tilde{\varphi}(x_N)$ in its boundary and that the N^{th} leg terminate at $\tilde{\varphi}(x_N)$. We need to restrict to a subset of Ω in order to define the final leg and foot.

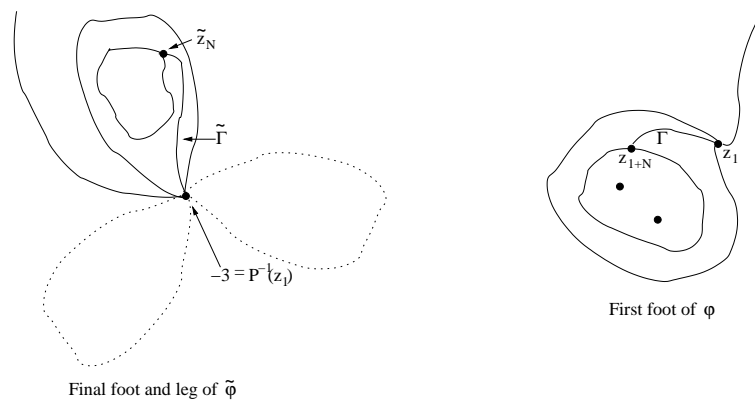


Figure 4.5: Demonstration of the trimming process.

By univalence, $\varphi(\mathcal{A})$ is a well-defined annulus in $\varphi(D_1)$, which has $\varphi(x_1)$ on its outer boundary, $\varphi(x_{1+N})$ on its inner boundary, and no distinguished points $\varphi(x_{1+kN})$ inside. Let $\tilde{\mathcal{A}}$ be the preimage of $\varphi(\mathcal{A})$ in Ω . Since we are pulling back by an analytic map, $\tilde{\mathcal{A}}$ contains none of the preimages of the distinguished points of $\varphi(D_1)$, but has $-d$ on its outer boundary and $\tilde{\varphi}(x_N)$ on its inner boundary. Set $\tilde{\varphi}(D_N) = \text{closure}(\Omega) - \text{closure}(\tilde{\mathcal{A}})$. Further, $\varphi(\Gamma)$ lifts to a well-defined path,

$\tilde{\Gamma}$, from $-d$ to $\tilde{\varphi}(x_{1+N})$. Set $\tilde{\varphi}(L_N) = \tilde{\Gamma} \cup \gamma$. Figure 4.5 illustrates the process of defining the final foot and leg.

Thus, we have completely specified a new spider $\tilde{\varphi}$ by pulling back via P and restriction. This defines a holomorphic mapping from $T_{\theta,\mu}^0$ to itself, which descends to a holomorphic self-mapping, σ_ℓ , of $\mathcal{T}_{\theta,\mu}$. It is easy to check that the equivalence class of $\tilde{\varphi}$ depends only on the equivalence class of φ . Figure 4.6 illustrates the complete pull-back picture.

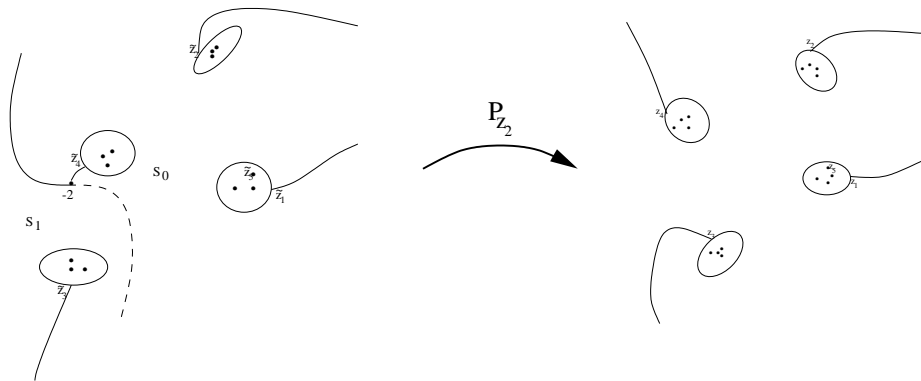


Figure 4.6: Spider map for $d = 2, \theta = \frac{3}{15}, \mu = 0.5i$

4.4 Characterization of Spider Maps

Earlier, when defining the standard spider, we incorporated a path Γ looping ℓ times through the annulus \mathcal{A} and we used this path in defining a spider mapping. We will show that for each ℓ , we get a different fixed spider class for σ_ℓ and hence, there are infinitely many spider mappings on our Spider space. At first glance, this seems a bit disconcerting since we are trying to use the iteration of a spider map to find the $d - 1$ parameters that lie above μ . As it turns out, for all l in the same congruence

class $\text{mod } (d - 1)$, the maps σ_ℓ all determine the same parameter. And so, the $d - 1$ classes of loops determine the full set of $d - 1$ parameters.

Theorem 4.4.1. *Let ℓ denote the looping of Γ . The fixed spider, $[\varphi_\ell]$ for σ_ℓ , consists of spiders whose legs loop about their respective feet $\frac{d}{d-1}\ell$ times. Thus, for each congruence class of $\ell \text{ mod } (d-1)$, the fixed spider φ_ℓ determines a unique parameter λ_ℓ .*

Proof. Begin with any spider φ_0 with interior looping number ℓ and analyze the effect of iteration of σ_ℓ on the looping. The key to this proof is that the interior looping eventually becomes looping outside the feet.

Suppose that the j^{th} leg of φ_0 spirals k_j times about the j^{th} foot and apply σ_ℓ once. This results in a new spider φ_1 such that, for $j = 1, \dots, N - 1$, the j^{th} leg spirals k_{j+1} times around the j^{th} foot and the N^{th} leg wraps $(\frac{k_1}{d} + \ell)$ times about the N^{th} foot. This follows from the fact that when pulling back via $P_{\varphi_0(x_2)}(z)$, the k_1 loops about the critical value 0 become $\frac{k_1}{d}$ loops about the preimage of $\varphi_0(D_1)$, and then the spider map adds the ℓ loops going from $-d$ to $\varphi_1(x_N)$. After N iterations, the j^{th} leg of $\varphi_N = \sigma_\ell^{\circ N}(\varphi_0)$ spirals $(\frac{k_j}{d} + \ell)$ times about the j^{th} foot. Continuing, we find that after mN iterations, the j^{th} leg wraps $\frac{k_j}{d^m} + \sum_{n=0}^{m-1} (\frac{1}{d})^n \ell$ times about the j^{th} foot. Taking the limit as $m \rightarrow \infty$, we see that the fixed spider $\varphi_{\infty, \ell}$ for σ_ℓ has each leg wrapping about its respective foot $\sum_{n=0}^{\infty} (\frac{1}{d})^n \ell = \frac{d}{d-1}\ell$ times. (Note that the wrapping of the legs about the feet in the initial spider is irrelevant as these loops are destroyed in the limit.) Setting $\lambda_\ell = \varphi_{\infty, \ell}(x_2)$, we get one of the $d - 1$ parameters lying above μ .

Next, suppose $\sigma_{\ell'}$ and σ_ℓ determine the same parameter, $\lambda = \varphi_{\infty, \ell'}(x_2) =$

$\varphi_{\infty,\ell}(x_2)$. Then, by induction, we get $\varphi_{\infty,\ell'}(x_n) = \varphi_{\infty,\ell}(x_n)$ for all $n \geq 3$. In particular, $\varphi_{\infty,\ell'}$ and $\varphi_{\infty,\ell}$ agree on the distinguished points in each foot, D_i , of the standard spider. Since each of these distinguished sequences has an accumulation point in the foot and both $\varphi_{\infty,\ell'}$ and $\varphi_{\infty,\ell}$ are analytic on the feet, it follows that these two maps agree on the $\bigcup D_i$. In other words, the feet for $\varphi_{\infty,\ell'}$ are the same as those for $\varphi_{\infty,\ell}$. The only way for two fixed spiders to have the same feet is if $\frac{d}{d-1}\ell'$ is congruent to $\frac{d}{d-1}\ell$ modulo d and this is equivalent to $\ell' \equiv \ell \pmod{d-1}$.

□

4.5 Fixed Points of Spider Maps

The following result shows that a fixed point of the spider map gives us a parameter λ such that $P_\lambda(z)$ has an attracting periodic cycle of a given length (equal to the period of θ under the d -tupling map) with multiplier μ . Actually, we do much better than this. The combinatorics of the fixed spider is also determined.

Theorem 4.5.1. *Suppose that $[\varphi]$ is a fixed point of σ_ℓ . Let φ be any representative of $[\varphi]$ and set $\lambda = \varphi(x_2)$. If $\zeta := \lim_{k \rightarrow \infty} \varphi(x_{1+kN})$, then*

$$P_\lambda^{\circ N}(\zeta) = \zeta \quad \text{and} \quad (P_\lambda^{\circ N})'(\zeta) = \mu.$$

Moreover, the portion of the j^{th} leg of the fixed spider outside $K_{P_{d,\lambda}}$ is homotopic to the dynamic ray of angle $d^{j-1}\theta$.

Proof. By assumption, we have that $[\tilde{\varphi}] = \sigma_\ell([\varphi])$, and so, $\tilde{\varphi}(x_j) = \varphi(x_j)$, for all $j \geq 1$. By construction, we have that $P_\lambda(\tilde{\varphi}(x_j)) = \varphi(x_{j+1})$, for all $j \geq 1$. So,

$$\begin{aligned}
P_\lambda^{\circ N}(\zeta) &= P_\lambda^{\circ N}\left(\lim_{k \rightarrow \infty} \varphi(x_{1+kN})\right) \\
&= P_\lambda^{\circ N}\left(\lim_{k \rightarrow \infty} \tilde{\varphi}(x_{1+kN})\right) \\
&= \lim_{k \rightarrow \infty} P_\lambda^{\circ N}(\tilde{\varphi}(x_{1+kN})) \\
&= \lim_{k \rightarrow \infty} \varphi(x_{1+(k+1)N}) \\
&= \zeta.
\end{aligned}$$

Next, we note that the fixed spider that we have found gives us a linearizing map for the target polynomial. In particular,

$$\varphi^{-1}|_{\varphi(D(\zeta, |\mu|r))} \circ P_{\varphi(x_2)}^{\circ N} \circ \varphi|_{\varphi^{-1}(D(\zeta, r))} = \mu$$

where r is chosen so that we are in a linearizing neighborhood of ζ . Thus, $P_{\varphi(x_2)}^{\circ N}$ has derivative μ at ζ .

In order to verify the second statement of the theorem, note that any looping of a leg of the fixed spider about its foot may be pushed inside of the Fatou component that contains the foot. This follows from the proof of Theorem 4.4.1 in which we show that any looping depends only on the looping that occurs in the annulus $\mathcal{A} \subset \varphi(D_1)$, which in turn is contained in the interior of $K_{P_{d,\lambda}}$. Hence, the portion of the j^{th} leg outside of the filled-in Julia set stretches to infinity like a dynamic ray and in fact, it is not difficult to see that this leg is homotopic to the union of the ray that lands at the characteristic repelling periodic point on the boundary of the Fatou components containing the j^{th} foot and the looping within the Fatou component.

□

Chapter 5

Complex Analytic Structure of Spider Space

In this chapter we show that Spider Space $\mathcal{T}_{\theta,\mu}$ is a complex manifold, by showing that it is isomorphic to a classical Teichmüller space as described in Chapter 3. Results there then show that Spider space has a unique analytic structure.

5.1 Analytic Structure of Spider Space

Let $\Omega = \mathbb{C} - \bigcup D_j$, which is a connected open subset of the sphere with N disjoint boundary circles. Clearly there is a mapping

$$M(\Omega) \rightarrow \mathcal{T}_{\theta,\mu} \quad \text{given by} \quad \nu \mapsto [\varphi^\nu]$$

where φ^ν is quasiconformal outside of the feet, sends x_1 to 0, fixes infinity, and is conformal on the feet. The equivalence relation here is the spider equivalence

relation which is $\varphi_1 \sim \varphi_2$ if there is a non-zero constant λ such that $\varphi_1 = \lambda\varphi_2$ on $\bigcup D_j$ and φ_1 is isotopic to $\lambda\varphi_2$ rel $\varphi_1(\bigcup D_j)$.

The Riemann surface Ω also has its own Teichmüller space in the classical sense, denoted $T(\Omega)$.

Theorem 5.1.1. *Spider space is isomorphic to $T(\Omega)$.*

Proof. There is a map $\Phi : \mathcal{T}_{\theta,\mu} \rightarrow T(\Omega)$ given by $\Phi([\varphi]) = [\varphi|_{\Omega}]$. In other words, we restrict the spider φ to Ω and consider its equivalence class in $T(\Omega)$. Clearly, this map is surjective. To see that this map is well-defined note that if φ_1 and φ_2 are spider equivalent, then their restrictions to Ω are isotopic rel the topological boundary which coincides with the ideal boundary in this case and hence they are equivalent in $T(\Omega)$.

Finally, suppose that $\Phi([\varphi_1]) = \Phi([\varphi_2])$ so that there is a analytic map g such that $g \circ \varphi_1 = \varphi_2$ on $\partial\Omega$ and $g \circ \varphi_1|_{\Omega}$ is isotopic to $\varphi_2|_{\Omega}$ rel $\partial\Omega$. We need to show that φ_1 and φ_2 are spider equivalent.

Since $\varphi_1(x_1) = \varphi_2(x_1) = 0$ and $\varphi_1(\infty) = \varphi_2(\infty) = \infty$, it follows that $g(0) = 0$ and $g(\infty) = \infty$. Extend g to \mathbb{C} by setting $g = \varphi_2 \circ \varphi_1^{-1}$ in $\mathbb{C} - \Omega$. Then, g is a homeomorphism on $\mathbb{C} - \partial\Omega$ and since $\partial\Omega$ is removable (as the disjoint union of circles), g is a global conformal homeomorphism. Since g fixes 0 and ∞ , it follows that $g(z) = cz$, for some non-zero $c \in \mathbb{C}$. So, we have that $\varphi_1 = (1/c)\varphi_2$ on $\mathbb{C} - \Omega$ and φ_1 is isotopic to $(1/c)\varphi_2$ rel $\mathbb{C} - \Omega$. Hence, φ_1 and φ_2 are Spider equivalent. \square

Thus, Spider space has the analytic structure of a Banach manifold.

5.2 The Tangent Space to Spider Space

We now describe the tangent space to spider space by examining the tangent vectors to a holomorphically varying curve of spiders. We will find two characterizations of the tangent space, which will provide a fruitful way of examining the spider map. Our first characterization involves a particular condition on vector fields.

Definition 5.2.1. *Let Z_φ be the space of complex-valued vector fields V on $\bigcup \varphi(\overline{D_j})$ which have continuous extensions \hat{v} to $\hat{\mathbb{C}}$ satisfying*

1. $\partial \hat{V} / \partial \bar{z}$ is bounded
2. \hat{V} is holomorphic on $\bigcup \varphi(D_j)$
3. $\hat{V}(0) = 0$ and
4. $\frac{\hat{V}}{z^2} \rightarrow 0$ as $z \rightarrow \infty$.

These conditions reflect the fact that each spider sends x_1 to 0 and fixes infinity. Hence, the vector fields generated as the feet move will have fix 0 and infinity.

We call Z_φ the space of *Zygmund bounded vector fields* on the feet of a spider. This space is a complex Banach space when equipped with the norm:

$$\|V\|_T := \inf \left\{ \|\bar{\partial} \hat{V}\|_\infty : \hat{V} \text{ is a continuous extension with bounded } \bar{\partial} - \text{derivative} \right\}.$$

Proposition 5.2.2. *The tangent space to Spider Space at $[\varphi]$, denoted $T_\varphi \mathcal{T}_{\theta, \mu}$, is Z_φ / \mathbb{C} , the space of Zygmund vector fields modulo the vector fields $cz \frac{\partial}{\partial z}$.*

Proof. Let φ_t , for $|t| < 1$, be a holomorphic curve of spiders such that $\varphi_0 = \varphi$. As t varies, this holomorphic curve defines a holomorphic motion, $\Phi(t, z) = (\varphi_t \circ \varphi^{-1})(z)$

of the feet, $\varphi(\cup \overline{D_j})$. Note that Φ fixes the points 0 and ∞ . By Slodkowski's Theorem, this holomorphic motion extends to a holomorphic motion $\hat{\Phi}_t$ of the entire Riemann sphere and the quasiconformal maps $\hat{\Phi}_t$ have Beltrami coefficients μ_t which depend holomorphically on t . Differentiating this curve of Beltrami coefficients, we have $\mu_t(z) = t\mu_0(z) + o(t)$ where $\mu_0 = \overline{\partial}\hat{V}$ and \hat{V} is the tangent vector to $\hat{\Phi}_t$ at $t = 0$. Thus, the tangent vector at the spider φ is given by restricting \hat{V} to the feet of φ . Hence, tangent vectors to φ give rise to vector fields on the sphere which have bounded $\overline{\partial}$ -derivative. Since the holomorphic motion fixes 0 and ∞ , these vector fields necessarily vanish at these points. Conversely, given a vector field $V(z)\frac{\partial}{\partial z}$ on the feet of the spider, which has an extension to the sphere with bounded $\overline{\partial}$ -derivative, the holomorphic dependence of solutions to the Beltrami differential equation implies that there is a holomorphic motion of the feet with $V(z)\frac{\partial}{\partial z}$ as the tangent vector field. \square

Next, we provide the second characterization of the tangent space, which is the Banach dual of a certain space of quadratic differentials on the sphere.

Definition 5.2.3. *Define Q_φ as the space of integrable quadratic differentials on the Riemann sphere, holomorphic on $\mathbb{C} - \bigcup \varphi(\overline{D_j})$.*

Proposition 5.2.4. *Q_φ is a Banach space with respect to the L^1 -norm on \mathbb{C} .*

Proof. Note that the disjointness of the $\varphi(d_j)$ implies that $\hat{\mathbb{C}} - \bigcup \varphi(\overline{D_j})$ is a open connected subset of $\hat{\mathbb{C}}$, and hence has a Riemann surface structure. So, we have the decomposition

$$Q_\varphi = L^1(\bigcup \varphi(\overline{D_j})) \oplus Q(\hat{\mathbb{C}} - \bigcup \varphi(\overline{D_j})).$$

Since $L^1(\bigcup \varphi(\overline{D_j}))$ and $Q(\hat{\mathbb{C}} - \bigcup \varphi(\overline{D_j}))$ are Banach spaces, it follows that Q_φ is also a Banach space. \square

Proposition 5.2.5. $Z_\varphi \cong Q_\varphi^*$, where Q_φ^* is the Banach dual of Q_φ .

Proof. To realize this, we use two results from functional analysis: the Hahn-Banach theorem and the Riesz Representation theorem.

Clearly, Q_φ can be identified as a closed subspace of $L^1(\mathbb{C})$. If ℓ is any bounded linear functional on Q_φ , then by Hahn-Banach, ℓ extends to a bounded linear functional, $\hat{\ell}$, on all of $L^1(\mathbb{C})$. By Riesz Representation, $\hat{\ell}$ is represented by an L^∞ function μ . By a well-known formula, we can solve $\bar{\partial}\hat{V} = \mu$ to find

$$\hat{V}(z) = -\frac{1}{\pi} \iint_{\mathbb{C}} \mu(\zeta) \left\{ \frac{1}{\zeta - z} - \frac{z}{\zeta - 1} + \frac{z - 1}{\zeta} \right\} |d\zeta|^2.$$

Letting V be the restriction of \hat{V} to the feet $\bigcup \varphi(\overline{D_j})$, we have a vector field $V(z) \frac{\partial}{\partial z}$ defined in Z_φ . Then, the correspondence $\ell \mapsto V$ gives an isomorphism between Q_φ^* and Z_φ . \square

Note that we have used the natural pairing between $L^1(\mathbb{C})$ and $L^\infty(\mathbb{C})$ to define the pairing

$$\begin{aligned} \langle , \rangle : \quad Z_\varphi \times Q_\varphi &\rightarrow \mathbb{C} \\ (V, q) &\mapsto \iint_{\mathbb{C}} \bar{\partial}\hat{V}(z)q(z)dz d\bar{z} \end{aligned} \quad (5.1)$$

where \hat{V} is any continuous extension of V .

Lemma 5.2.6. *The value of the integral in (5.1) does not depend on the choice of extension \hat{V} .*

Proof. See [19]. □

Summarizing, we have the following identifications: $T_\varphi \mathcal{T}_{\theta, \mu} = Z_\varphi = Q_\varphi^*$.

Even though Q_φ is not reflexive, it is separable with Rat_φ , the rational elements in Q_φ , as a dense subspace. More precisely,

Definition 5.2.7. *Rat_φ is the Banach space of holomorphic quadratic differentials on $\hat{\mathbb{C}}$ with, at worst, simple poles at a finite number of points of $\bigcup \varphi(\overline{D_j})$.*

Proposition 5.2.8. *Rat_φ is dense in Q_φ .*

Proof. This fact is known as Bers' Approximation Theorem and a complete proof is found in [13], Chapter 3. □

An element $q \in Rat_\varphi$ has the form

$$q(z)dz^2 = \left(\sum_{k=1}^m \frac{c_k}{z - p_k} \right) dz^2,$$

where $p_k \in \bigcup \varphi(\overline{D_j})$. Further, for $q \in Rat_\varphi$, the above pairing takes a more explicit form:

$$\langle V, q \rangle = \iint_{\mathbb{C}} \bar{\partial} \hat{V}(z) q(z) |dz|^2 = 2\pi i \sum_{k=1}^m \text{Res}_{p_k} V q. \quad (5.2)$$

Chapter 6

Contraction of the Spider Map

Having identified the tangent space, the derivative of the spider map is a linear mapping $d_\varphi \sigma_\ell : T_\varphi \mathcal{T}_{\theta, \mu} \rightarrow T_{\tilde{\varphi}} \mathcal{T}_{\theta, \mu}$, where $[\tilde{\varphi}] = \sigma_\ell([\varphi])$. In this section we show that this mapping is strictly contracting in norm, thus allowing us a way to iterate to a fixed point of the spider map. Of course, proving contraction requires a metric on Spider Space. We define an infinitesimal metric that is defined on the tangent space to Spider Space. In fact, this metric is dual to the L^1 norm on Q_φ and we will work with a push-forward operator on Q_φ and show that this operator is the adjoint of the derivative $d_\varphi \sigma_\ell$.

6.1 The Push-forward Operator

We begin with the description of this dual map, $P_* : Q_{\tilde{\varphi}} \rightarrow Q_\varphi$, which is the pushforward operator with respect to the polynomial $P = P_{\varphi(x_2)}$. More precisely, let z_0 be any non-zero point on the Riemann sphere and take U to be any simply

connected open neighborhood of z_0 which does not contain zero. Then, $P^{-1}(U)$ consists of d domains, V_1, V_2, \dots, V_d , which have disjoint closures. Given $\tilde{q} \in Q_{\tilde{\varphi}}$, define

$$P_*(\tilde{q}) = \sum_{i=1}^d \tilde{q}_i \text{ on } U$$

where $\tilde{q}_i = \tilde{q}|_{V_i}$. Clearly, $P_*(\tilde{q})$ is holomorphic on $\hat{\mathbb{C}} - \bigcup \varphi(\overline{D_j})$, possibly gaining poles on $\bigcup \varphi(\overline{D_j})$ at the images of poles of \tilde{q} . As always, the operator norm of the mapping P_* is given by

$$\|P_*\| = \sup_{\tilde{q} \in Q_{\tilde{\varphi}}, \|\tilde{q}\|_1 = 1} \|P_*(\tilde{q})\| \quad (6.1)$$

Integrability of $P_*(\tilde{q})$ and the bound on the norm of P_* follows from:

$$\int_U |P_*(\tilde{q})| \leq \sum_{i=1}^d \int_{V_i} |\tilde{q}_i| = \int_{P^{-1}(U)} |\tilde{q}| < \infty$$

Thus, $P_*(\tilde{q})$ is integrable and $\|P_*\| \leq 1$. We now eliminate the case $\|P_*\| = 1$.

Proposition 6.1.1. *P_* is strictly contracting; that is, $\|P_*\| < 1$.*

Proof. Suppose that $\|P_*\| = 1$. Then, there is a sequence $\tilde{q}_n \in Q_{\tilde{\varphi}}$, each of norm 1, such that $\|P_*(\tilde{q}_n)\|_1 \nearrow 1$ as $n \rightarrow \infty$.

First, we eliminate the case in which a particular \tilde{q} realizes a pushforward norm of 1; that is, we show that $\|P_*(\tilde{q})\|_1 = 1$ is impossible. Let $z \neq 0$ be any point of the Riemann sphere marked by φ . Then, z has d preimages: \tilde{z} , the image of z under the spider map, and $d - 1$ other points $\tilde{w}_2, \dots, \tilde{w}_d$. Now, \tilde{q} cannot have poles at the $\{\tilde{w}_i\}_{i=2}^d$ since, by definition of the spider map, the \tilde{w}_i live outside the feet of $\tilde{\varphi}$. Choosing an open neighborhood U of z , we see that $\|P_*(\tilde{q})\|_1 = 1$ implies that

equality holds in the triangle inequality above and hence, $\tilde{q}_1 = k \sum_{i=2}^d \tilde{q}_i$, for some $k \geq 0$. But the \tilde{q}_i , for $i \geq 2$, have no poles at the \tilde{w}_i , and so \tilde{q} has no pole at \tilde{z} .

Putting all this together, we see that \tilde{q} is a holomorphic quadratic differential on the Riemann sphere with possibly simple poles at $-d$ and ∞ only. But, any such quadratic differential must have at least four poles. This contradiction tells us that $\|P_*(\tilde{q}_n)\|_1 < 1$ for each n .

Since each $q_n := P_*(\tilde{q}_n)$ is uniformly bounded, $\{q_n\}$ forms a normal family and hence, we can extract a convergent subsequence q_{n_k} which converges to $q \in Q_\varphi$. Using Fatou's lemma, we find that

$$\|q\|_1 = \int \liminf_{k \rightarrow \infty} |q_{n_k}| \leq \liminf_{k \rightarrow \infty} \int |q_{n_k}| = 1$$

Also note that, since the \tilde{q}_n all have norm 1, we can extract a convergent subsequence that converges to some \tilde{q} with $\|\tilde{q}\|_1 = 1$. So, we have $\tilde{q}_n \rightarrow \tilde{q}$ and $P_*\tilde{q}_n \rightarrow q \in Q_\varphi$. Since P_* is a bounded operator, it is closed, and so, we get $\tilde{q} \in Q_{\tilde{\varphi}}$ and $P_*\tilde{q} = q$. By Fatou's lemma, we showed that $\|q\|_1 \leq 1$. If $\|q\|_1 = 1$, then we have $1 = \|\tilde{q}\|_1 \geq \|P_*\tilde{q}\|_1 = \|q\|_1 = 1$. This forces $\|P_*\tilde{q}\|_1 = \|\tilde{q}\|_1$, which contradicts our earlier argument. Thus, we must have $\|q\|_1 < 1$, and hence, our original sequence could not converge to 1. So, $\|P_*\| < 1$. \square

Now, we have shown that the mapping P_* is strictly contracting and once we show that P_* is dual to $d_\varphi\sigma_\ell$, we will have proved the claim that $d_\varphi\sigma_\ell$ is strictly contracting. Before we prove the duality, we obtain an explicit expression for the derivative of the spider mapping.

6.2 Derivative of the Spider Map

If $\tilde{z} \in \tilde{\varphi}(\overline{D}_j)$, then $z = P_{z_2}(\tilde{z}) \in \varphi(\overline{D}_{j+1})$, where $z_2 = \varphi(x_2)$. Differentiating the equation

$$z = P_{z_2}(\tilde{z}) = z_2 \left(1 + \frac{\tilde{z}}{d}\right)^d,$$

we find:

$$V_{j+1}(z) = V_2(z_2) \left(1 + \frac{\tilde{z}}{d}\right)^d + z_2 \left(1 + \frac{\tilde{z}}{d}\right)^{d-1} \tilde{V}_j(\tilde{z})$$

where $V(z) \frac{\partial}{\partial z} \in Z_\varphi$ and $V_{j+1}(z) = V|_{\varphi(\overline{D}_{j+1})}(z)$ is a tangent vector anchored at z . (Similar statements hold for $\tilde{V} \frac{\partial}{\partial \tilde{z}} \in Z_{\tilde{\varphi}}$.) So to determine the tangent vector anchored at \tilde{z} , we need only solve for $\tilde{V}_j(\tilde{z})$, giving

$$\begin{aligned} \tilde{V}_j(\tilde{z}) &= \frac{1}{z_2 \left(1 + \frac{\tilde{z}}{d}\right)^{d-1}} \left[V_{j+1}(z) - V_2(z_2) \left(1 + \frac{\tilde{z}}{d}\right)^d \right] \\ &= (d_{\tilde{z}} P_{z_2})^{-1} V_{j+1}(z) - \frac{V_2(z_2)}{z_2} \left(1 + \frac{\tilde{z}}{d}\right) \end{aligned}$$

Let $v_j(z) = (d_{\tilde{z}} P_{z_2})^{-1} V_{j+1}(z)$ be the vector field obtained by lifting the V via the derivative of P_{z_2} and let

$$\nu(\tilde{z}) = \frac{V_2(z_2)}{z_2} \left(1 + \frac{\tilde{z}}{d}\right)$$

be the global vector field that vanishes at $-d$ and infinity and has value

$$\frac{V_2(z_2)}{z_2}$$

at 0. Then, we write

$$\tilde{V}_j(\tilde{z}) = v_j(z) - \nu(\tilde{z}).$$

The reason for the adjustment by the vector field ν is the same as is explained in [15]. One might expect that the derivative of a spider mapping would simply lift

the vector field V to \tilde{V} via P_{z_2} . The problem with this is that the tangent vector at 0 may fail to vanish even though 0 is fixed under the spider mapping. Thus, we need to correct the lifted vector field by the global vector ν .

Lemma 6.2.1. *The mapping $P_* : Q_{\tilde{\varphi}} \rightarrow Q_{\varphi}$ is dual to $d_{\varphi}\sigma_{\ell} : T_{\varphi}\mathcal{T}_{\theta,\mu} \rightarrow T_{\tilde{\varphi}}\mathcal{T}_{\theta,\mu}$.*

Proof. Let $V \in Z_{\varphi}$ and $\tilde{q} \in Q_{\tilde{\varphi}}$. Since $Rat_{\tilde{\varphi}}$ is dense in $Q_{\tilde{\varphi}}$, we may assume that $q \in Rat_{\tilde{\varphi}}$ in order to prove the lemma. We must show that

$$\langle (d_{\varphi}\sigma_{\ell})(V), \tilde{q} \rangle = \langle V, P_*(\tilde{q}) \rangle .$$

Let $\tilde{p}_1, \tilde{p}_2, \dots, \tilde{p}_m$ be the finitely many poles of \tilde{q} . Then,

$$\begin{aligned} \frac{1}{2\pi i} \langle \tilde{V}, \tilde{q} \rangle &= \sum_{k=1}^m \text{Res}_{\tilde{p}_k} \tilde{V} \tilde{q} \\ &= \sum_{k=1}^m \sum_{j=1}^N \text{Res}_{\tilde{p}_k} \tilde{V}_j \tilde{q} \\ &= \sum_{k=1}^m \left(\sum_{j=1}^N \text{Res}_{\tilde{p}_k} v_j \tilde{q} - \sum_{j=1}^N \text{Res}_{\tilde{p}_k} \nu \tilde{q} \right) \\ &= \sum_{k=1}^m \sum_{j=1}^N \text{Res}_{\tilde{p}_k} v_j \tilde{q}. \end{aligned} \tag{6.2}$$

The second summation in (6.2) vanishes by Cauchy's formula since $\nu \tilde{q}$ is a global 1-form on the sphere. Next, let $p_k = P_{z_2}(\tilde{p}_k)$. From the definition of the push-forward, we have

$$\begin{aligned} \frac{1}{2\pi i} \langle V, P_* \tilde{q} \rangle &= \sum_{k=1}^m \text{Res}_{p_k} V \cdot P_* \tilde{q} \\ &= \sum_{k=1}^m \sum_{j=1}^N \text{Res}_{\tilde{p}_k} v_j \tilde{q} + \sum_{i=1}^{d-1} \sum_{k=1}^m \sum_{j=1}^N \text{Res}_{\tilde{w}_k^{(i)}} \hat{v}_j \tilde{q}, \end{aligned}$$

where $\tilde{w}_k^{(i)}$ is one of the $d - 1$ pre-images of p_k which does not lie in any foot of $\tilde{\varphi}$ and $\hat{v}_j = (d_{\tilde{w}_k^{(i)}} P_{z_2})^{-1} V_{j+1}$. Since \tilde{q} does not have a pole at any of the $\tilde{w}_k^{(i)}$ and \hat{v}_j is holomorphic, the triple sum in the last computation vanishes. Thus,

$$\langle V, P_* \tilde{q} \rangle = 2\pi i \sum_{k=1}^m \sum_{j=1}^N \text{Res}_{\hat{p}_k} v_j \tilde{q} = \langle \tilde{V}, \tilde{q} \rangle .$$

□

Combining Lemma 6.1.1 and Lemma 6.2.1, we have

Proposition 6.2.2. (Spider Contraction)

The Spider mapping is strongly contracting. That is, $\|d_\varphi \sigma_\ell\| < 1$.

6.3 Convergence of the Algorithm

In this section, we define a subset of spiders which is invariant under the spider map and show that Spider Space is attracted to this invariant set. This compactness statement is a bit complicated and may seem confusing. The point is that we find a set of spiders for which the feet remain bounded away from infinity and do not shrink to points under iteration. We verify that the sequence $\varphi_n(x_2) = (\sigma^{on}(\varphi))(x_2)$ does not converge to 0. These conditions depend most definitely on the fact that the multiplier of our target map is in the punctured disc.

Since the polynomial we seek will have an attracting cycle of multiplier μ with $0 < |\mu| < 1$, the orbit of 0 is infinite and discrete. Hence, there is a closest return of 0 under iteration of the target polynomial. Let $C(\mu)$ denote this distance. Then, we have

Proposition 6.3.1. (Invariant Subset)

Let $0 < \epsilon < C(\mu)/2$ and define $\mathcal{T}_{\theta,\mu}^\epsilon \subset \mathcal{T}_{\theta,\mu}$ as the set of spiders, φ satisfying

- (i) $\varphi(x_j) \in D\left(-d, d\left(\frac{2d}{\epsilon}\right)^{\frac{1}{d-1}}\right)$, for $j \geq 1$,
- (ii) the discs $D(\varphi(x_j), \epsilon^j)$, for $j \geq 1$, are disjoint.

Then, $\mathcal{T}_{\theta,\mu}^\epsilon$ is invariant under the spider mappings of $\mathcal{T}_{\theta,\mu}$.

Proof. Let φ be any spider satisfying (i) and (ii) above. We show that $\tilde{\varphi} = \sigma(\varphi)$ also satisfies these conditions. We verify condition (i) first.

Since $\varphi(x_{j+1}) \in D\left(-d, d\left(\frac{2d}{\epsilon}\right)^{\frac{1}{d-1}}\right)$, we have

$$|\varphi(x_{j+1})| < d + d\left(\frac{2d}{\epsilon}\right)^{\frac{1}{d-1}}. \quad (6.3)$$

We also know that $|\varphi(x_2)| > \epsilon$, by condition (ii) as $\varphi(x_1) = 0$. So,

$$\begin{aligned} |\tilde{\varphi}(x_j) + d| &= |P_{\varphi(x_2)}^{-1}(\varphi(x_{j+1})) + d| \\ &= d \frac{|\varphi(x_{j+1})|^{\frac{1}{d}}}{|\varphi(x_2)|^{\frac{1}{d}}} \\ &< d \frac{|\varphi(x_{j+1})|^{\frac{1}{d}}}{\epsilon^{\frac{1}{d}}} && \text{as } |\varphi(x_2)| > \epsilon \\ &< \frac{d}{\epsilon^{\frac{1}{d}}} \left(d + d \left(\frac{2d}{\epsilon} \right)^{\frac{1}{d-1}} \right)^{\frac{1}{d}} && \text{by (6.3)} \\ &< d \left(\frac{d}{\epsilon} + \frac{d}{\epsilon} \left(\frac{2d}{\epsilon} \right)^{\frac{1}{d-1}} \right)^{\frac{1}{d}} \\ &< d \left(\frac{2d}{\epsilon} \right)^{\frac{1}{d-1}} && \text{by Lemma 6.3.2 below.} \end{aligned}$$

In order to verify that condition (ii) holds for $\tilde{\varphi}$, we first show that the points $\tilde{\varphi}(x_j)$ stay a bounded distance away from $-d$. Note that $P_{\varphi(x_2)}^{-1}(D(0, \epsilon))$ is a disc

centered at $-d$ with radius

$$|P_{\varphi(x_2)}^{-1}(\epsilon) + d| = d \frac{\epsilon^{\frac{1}{d}}}{|\varphi(x_2)|^{\frac{1}{d}}}.$$

Also, since $D(0, \epsilon)$ does not contain any of the points $\varphi(x_j)$, for $j \geq 2$, it follows that $P_{\varphi(x_2)}^{-1}(D(0, \epsilon))$ does not contain any of the $\tilde{\varphi}(x_j)$, for $j \geq 1$. So, if

$$|w + d| > d \frac{\epsilon^{\frac{1}{d}}}{|\varphi(x_2)|^{\frac{1}{d}}},$$

then

$$\begin{aligned} |P'_{\varphi(x_2)}(w)| &= \frac{|\varphi(x_2)|}{d^{d-1}} |w + d|^{d-1} \\ &> \frac{|\varphi(x_2)|}{d^{d-1}} \left(d \frac{\epsilon^{\frac{1}{d}}}{|\varphi(x_2)|^{\frac{1}{d}}} \right)^{d-1} \\ &= |\varphi(x_2)|^{\frac{1}{d}} \epsilon^{1-\frac{1}{d}} \\ &> \epsilon^{\frac{1}{d}} \epsilon^{1-\frac{1}{d}} \quad \text{as } |\varphi(x_2)| > \epsilon \\ &= \epsilon. \end{aligned}$$

Hence, for $|P_{\varphi(x_2)}^{-1}(z) + d| > d \frac{\epsilon^{\frac{1}{d}}}{|\varphi(x_2)|^{\frac{1}{d}}}$, we have

$$\left| \left(P_{\varphi(x_2)}^{-1} \right)'(z) \right| = \frac{1}{\left| P'_{\varphi(x_2)} \left(P_{\varphi(x_2)}^{-1}(z) \right) \right|} < \frac{1}{\epsilon}.$$

Then, if $z \in D\left(-d, d\left(\frac{2d}{\epsilon}\right)^{\frac{1}{d-1}}\right)$ lies within the disc of radius ϵ^{j+1} about z_{j+1} and $|z| > \epsilon$, then $\tilde{z} = P_{\varphi(x_2)}^{-1}(z)$ lies in a disc about $\tilde{\varphi}(x_j) = P_{\varphi(x_2)}^{-1}(\varphi(x_{j+1}))$ of radius $\frac{1}{\epsilon}\epsilon^{j+1} = \epsilon^j$. Clearly these preimage discs cannot intersect since their images did not intersect. \square

Lemma 6.3.2. *Let ϵ be as in Proposition 6.3.1. Then,*

$$\left(\frac{d}{\epsilon} + \frac{d}{\epsilon} \left(\frac{2d}{\epsilon} \right)^{\frac{1}{d-1}} \right)^{\frac{1}{d}} < \left(\frac{2d}{\epsilon} \right)^{\frac{1}{d-1}}.$$

Proof. Since $2d > \epsilon$, we have

$$\begin{aligned}
\frac{2d}{\epsilon} > 1 &\implies \left(\frac{2d}{\epsilon}\right)^{\frac{1}{d-1}} > 1 \\
&\implies \frac{1}{2} \left(\frac{2d}{\epsilon}\right)^{\frac{1}{d-1}} > \frac{1}{2} \\
&\implies \left(\frac{2d}{\epsilon}\right)^{\frac{1}{d-1}} > \frac{1}{2} + \frac{1}{2} \left(\frac{2d}{\epsilon}\right)^{\frac{1}{d-1}} \\
&\implies \frac{2d}{\epsilon} \left(\frac{2d}{\epsilon}\right)^{\frac{1}{d-1}} > \frac{d}{\epsilon} + \frac{d}{\epsilon} \left(\frac{2d}{\epsilon}\right)^{\frac{1}{d-1}} \\
&\implies \left(\frac{2d}{\epsilon}\right)^{\frac{d}{d-1}} > \frac{d}{\epsilon} + \frac{d}{\epsilon} \left(\frac{2d}{\epsilon}\right)^{\frac{1}{d-1}} \\
&\implies \left(\frac{2d}{\epsilon}\right)^{\frac{1}{d-1}} > \left(\frac{d}{\epsilon} + \frac{d}{\epsilon} \left(\frac{2d}{\epsilon}\right)^{\frac{1}{d-1}}\right)^{\frac{1}{d}}
\end{aligned}$$

□

This invariant subset is characterized by the fact that the distinguished points $\varphi(x_j)$ remain bounded way from each other. Actually, this is clear for the distinguished points that lie completely inside different feet, since by construction, $\varphi(D_i) \cap \varphi(D_j) = \emptyset$. For $\varphi \in \mathcal{T}_{\theta, \mu}^\epsilon$, we further know that, under iteration of the spider mapping, the points on the boundaries of the feet, namely $\varphi(x_1) = 0, \varphi(x_2), \dots, \varphi(x_N)$, do not coalesce and that the feet do not become arbitrarily small (in the Euclidean metric).

Now, we come to the main theorem of the thesis. This result is a version of Thurston's algorithm (see [9] or [15]) in which we do not have post-critical finiteness. First, we will need a lemma.

Lemma 6.3.3. *Let φ_0 and φ_1 be any two spiders in $\mathcal{T}_{\theta,\mu}^\epsilon$. Then, there exists $\delta > 0$ and a path γ connecting φ_0 to φ_1 and contained in $\mathcal{T}_{\theta,\mu}^\delta$.*

Proof. Note that $\varphi_0(\cup \overline{D}_j)$ and $\varphi_1(\cup \overline{D}_j)$ are all contained in the disc centered at $-d$ of radius $d \left(\frac{2d}{\epsilon}\right)^{\frac{1}{d-1}}$. Pull each feet of each spiders back along its leg until the last intersection of the leg with the circle $\left\{ |z + d| = d \left(\frac{2d}{\epsilon}\right)^{\frac{1}{d-1}} \right\}$. Now, move the feet into the standard position and we will have obtained a path connecting the two spiders. The distinguished points of the spiders, $\{\varphi_k(x_j)\}_{j \in \mathbb{N}, k=1,2}$, will remain bounded apart throughout this process and we may choose δ in terms of this distance. Further, all of the feet of the spiders along this path will stay within the disc centered at $-d$ of radius $d \left(\frac{2d}{\delta}\right)^{\frac{1}{d-1}}$. \square

Proposition 6.2.2 (on the strict contraction of the derivative) shows that at any spider the norm of the derivative is less than one, but this does not guarantee that we have global uniform contraction constant. We will show that the norm of the derivative depends only on the position in moduli space, which is the space of feet.

Consider the space $\mathcal{M}(\cup D_j)$ which is the set of maps $\varphi : \cup D_j \rightarrow \mathbb{C}$ which are univalent on $\cup D_j$, modulo the equivalence relation: $\varphi_1 \sim \varphi_2$ if $\varphi_2 = \lambda \varphi_1$ on $\cup D_j$. This is the moduli space of Spider Space and $\pi : \mathcal{T}_{\theta,\mu} \rightarrow \mathcal{M}(\cup D_j)$ is a universal covering space. $\mathcal{M}(\cup D_j)$ has the Teichmüller topology induced from the quotient map from Spider Space and since Spider Space is the universal covering of moduli space, the tangent space $T_\varphi \mathcal{T}_{\theta,\mu}$ is the same as $T_{\pi(\varphi)} \mathcal{M}(\cup D_j)$.

Let $\varphi \in \mathcal{T}_{\theta,\mu}^\delta$. After the first iteration of the spider mapping, $\sigma_{\theta,\mu}(\varphi) \in \mathcal{T}_{\theta,\mu}^\delta$ is univalent on $\cup D_j$. Note however, that prior to restriction to a subdisc, the spider algorithm produces a map that is univalent on a disc D'_N which compactly contains

D_N . As we iterate the spider mapping, this property (of restriction to subdiscs) propagates to the other feet. So, after N iterations, the feet of $\sigma_{\theta,\mu}^N(\varphi)$ is the restriction of a map ψ which is univalent on $\bigcup D'_j$ compactly containing $\bigcup D_j$. Further, since we are working in $\mathcal{T}_{\theta,\mu}^\delta$, Proposition 6.3.1 implies that the image of ψ is contained in a disc of fixed radius R about the origin and that $|\psi'(c_j)| > \epsilon'$, for some $\epsilon' > 0$, where c_j is the center of D_j . The delicate inequalities in Proposition 6.3.1 actually apply to the branches of $P_{\varphi(x_2)}^{-1}$ before the restriction by the spider mapping and so the estimates there apply to this space of univalent maps on the larger discs. Since this proposition provides a fixed compact set that contains the feet of all spiders in $\mathcal{T}_{\theta,\mu}^\delta$ and that all feet retain a definite fixed size under iteration, the conditions on ψ follow easily. When working in the invariant subset of Spider Space, the feet retain a definite size upon iteration of the spider mapping and so there is a definite positive derivative at the centers of the feet. Hence, the derivative condition for ψ follows. This argument is much in the spirit of the Koebe 1/4-Theorem.

The fact that the feet are compactly contained in bigger discs actually follows from the removal of annuli of fixed size. The spider mapping discards an annulus on each iteration based on the distance between points on the orbit of $\varphi(x_1) = 0$. Since we are working in $\mathcal{T}_{\theta,\mu}^\delta$ and Proposition 6.3.1 guarantees that the points along the orbit are separated from 0 by at least $\delta > 0$, the annulus that is removed has a definite fixed size.

Let $\Psi_{R,\epsilon'}$ be the space of univalent mappings $\psi : \bigcup D'_j \rightarrow \mathbb{C}$ such that the image of ψ is contained in D_R , the disc of radius R about the origin, and $|\psi'(c_j)| > \epsilon'$, where c_j is the center of D_j . Endowing this space with the topology of uniform convergence

on compact subsets, $\Psi_{R,\epsilon}$ is a compact space as is seen from the normalization conditions on $\psi \in \Psi_{R,\epsilon}$. This compactness is the same argument as in the proof of the compactness of the univalent maps of the unit to itself with the derivative at the origin normalized. We now come to one part of our compactness argument.

Lemma 6.3.4. *Consider the map $\alpha : \Psi_{R,\epsilon'} \rightarrow \mathcal{M}(\bigcup D_j)$ given by $\alpha(\psi) = \psi|_{\bigcup D_j}$. Then, α is a continuous map with respect to the topology of uniform convergence on $\Psi_{R,\epsilon'}$ and the Teichmüller topology on $\mathcal{M}(\bigcup D_j)$.*

Proof. In general, uniform convergence on compact subsets does not imply convergence in the Teichmüller topology since problems arise on the boundary of the discs D'_j . In this case, however, there is no problems at the boundaries of the D_j since we have the restriction of univalent mappings to compactly contained subdiscs of the D'_j . In fact, such a restriction is a compact mapping and we find that the restricted maps are analytic on the boundaries of the D_j (again by the fact that these discs are compactly contained in the D'_j .) \square

Next, consider the map $\tilde{\pi} : \mathcal{T}_{\theta,\mu}^\delta \rightarrow \Psi_{R,\epsilon}$ given by restriction to $\bigcup D'_j$. Note that this map is well-defined only after the N^{th} iterate of the spider mapping since prior to that we do not yet have the spider mapping as a restriction of univalent mappings on larger discs. Clearly, $\tilde{\pi}$ is the forgetful map that omits the combinatorial information and projects onto the D'_j . We now have

Lemma 6.3.5. *The image of $\mathcal{T}_{\theta,\mu}^\delta$ in moduli space is compact.*

Proof. After N iterations of the spider mapping, we have the following commutative

diagram

$$\begin{array}{ccc}
 \mathcal{T}_{\theta,\mu}^\delta & \xrightarrow{\sigma_{\theta,\mu}} & \mathcal{T}_{\theta,\mu} \\
 \tilde{\pi} \downarrow & & \downarrow \pi \\
 \Psi_{R,\epsilon'} & \xrightarrow{\alpha} & \mathcal{M}(\bigcup D_j)
 \end{array}$$

Again, it is important to realize that, after N iterations of the spider mapping, the spider algorithm produces mappings that are univalent on discs compactly containing the feet. Hence, the map $\tilde{\pi}$ is well-defined. Then, $U = \pi(\mathcal{T}_{\theta,\mu}^\delta) = \pi(\sigma(\mathcal{T}_{\theta,\mu}^\delta)) = \alpha(\tilde{\pi}(\mathcal{T}_{\theta,\mu}^\delta)) = \alpha(\Psi_{R,\epsilon'})$. Since $\Psi_{R,\epsilon'}$ is compact and α is continuous, it follows that $U = \alpha(\Psi_{R,\epsilon'})$ is compact. \square

So, while $\mathcal{T}_{\theta,\mu}^\delta$ is not compact, its image in moduli space is compact. Further, the norm of the derivative only depends on $\tilde{\pi}(\varphi)$ since the norm of the co-derivative P_* depended only on the preimages of the feet and hence the values on $\bigcup D_j'$. This is the content of Lemma 6.1.1. Thus, the derivative depends only on the geometric information encoded in the feet and the position in moduli space. Since we have seen that we are working in a compact subset of moduli space, our pointwise bound on the derivative will become a uniform bound.

Proposition 6.3.6. *There exists a constant $C_\delta < 1$ such that the norm of the derivative is bounded above by C_δ on all of $\mathcal{T}_{\theta,\mu}^\delta$.*

Proof. Since the norm of the derivative depends only on the position in moduli space and the image of $\mathcal{T}_{\theta,\mu}^\delta$ is compact in moduli space, we have that

$$C_\delta = \max_{\pi(\varphi) \in U} \|d_\varphi \sigma\| < 1.$$

The maximum is achieved since we are in a compact subset of moduli space. \square

Theorem 6.3.7. *Suppose that θ is periodic under $\theta \mapsto d\theta$ and that $0 < |\mu| < 1$. Then, for each $\ell \in \mathbb{Z}$, σ_ℓ has a unique fixed point which can be found under iteration of the spider mapping.*

Proof. Let $\varphi_0 \in \mathcal{T}_{\theta,\mu}^\epsilon$ and set $\varphi_m = \sigma_\ell^{\circ m}(\varphi_0)$ for $m \in \mathbb{N}$. By Lemma 6.3.3, there is a $\delta > 0$ and a path γ_0 such that γ_0 joins φ_0 and φ_1 and is contained in $\mathcal{T}_{\theta,\mu}^\delta$. Let L denote the length of γ_0 , which is finite as we may assume that γ_0 is a C^1 curve. Set $\gamma_m = \sigma_\ell^{\circ m}(\gamma_0)$. By Proposition 6.3.1, φ_m and γ_m lie in $\mathcal{T}_{\theta,\mu}^\delta$ for each m . By Proposition 6.3.6, there is a constant $C_\delta < 1$ such that $\text{length}(\gamma_m) < C_\delta^m L$. Thus, the spiders φ_m form a Cauchy sequence.

Note that the univalent maps $\varphi_m|_{D_j}$ are uniformly bounded by $d + d \left(\frac{2d}{\delta}\right)^{\frac{1}{d-1}}$, and hence, form a normal family. Thus, $\varphi_m|_{D_j}$ converges uniformly on compact subsets to a limit $\varphi_\infty|_{D_j}$ that is either constant or univalent. This limit cannot be constant since distinguished points in $\varphi_m(D_j)$ are uniformly bounded apart (independent of m).

□

With this theorem, we can answer Question 1 in the affirmative.

Corollary 6.3.8. *With θ, μ as in Theorem 6.3.7, there exists $d - 1$ polynomials $P_{\lambda_\ell, d}(z) = \lambda_\ell \left(1 + \frac{z}{d}\right)^d$ such that $P_{\lambda_\ell, d}$ has an (attracting) cycle of length equal to the period of θ with multiplier μ , and having the specified combinatorics from θ .*

Proof. By Theorem 6.3.7, there exists a unique fixed point $[\varphi_{\ell, \infty}]$ of σ_ℓ . By Theorem 4.5.1, we have a desired polynomial by setting $\lambda_\ell = \varphi_{\ell, \infty}(x_2)$. Finally, Theorem 4.4.1 implies that there are exactly $d - 1$ classes $[\varphi_{\ell, \infty}]$ determining the $d - 1$ polynomials.

□

Chapter 7

Extension to Exponentials

7.1 Introduction

In this chapter, we want to extend the generalized spider algorithm for polynomials to the family of mappings, $E_\lambda(z) = \lambda e^z$. In particular, we describe a variant of the algorithm, found in the previous chapters, which can be used to locate parameters within hyperbolic components of the parameter plane of E_λ .

7.2 Exponential Dynamics

We will later prove results about hyperbolic components of the parameter space for the family of mappings $E_\lambda(z) = \lambda e^z$. This section contains the basic theory of the iteration of exponential maps of the sphere, highlighting some of the similarities and differences between the iteration of rational maps and the iteration of exponentials. One of the main differences arises from the point at infinity. From a dynamical point

of view, ∞ is no different than another other point on the sphere when iterating polynomials, whereas ∞ is an essential singularity for $E_\lambda(z)$. By a theorem of Picard, we know that any neighborhood of ∞ is mapped over the entire plane by E_λ , missing at most one point, and taking all other values infinitely often. This is a stark contrast with polynomials.

As we have seen with rational dynamics, the critical points play a distinguished role in determining the dynamics of rational maps and the topology of their Julia sets. Since $E_\lambda(z)$ has no critical points, we look to *asymptotic values* to play the role that critical points played.

Definition 7.2.1. *Suppose that $f : \mathbb{C} \rightarrow \mathbb{C}$ is an entire transcendental function. A point $w \in \hat{\mathbb{C}}$ is called an asymptotic value for f if there exists a continuous curve $\gamma(t)$ such that*

$$\lim_{t \rightarrow \infty} \gamma(t) = \infty \quad \text{and} \quad \lim_{t \rightarrow \infty} f(\gamma(t)) = w.$$

For example, 0 is an asymptotic value for E_λ . We will also refer to 0 as the *singular value* for E_λ .

Theorem 7.2.2. *Suppose that f is an entire transcendental function and that z_0 lies on an attracting or parabolic cycle for f . Then, the orbit of at least one critical point or asymptotic value is attracted to the orbit of z_0 .*

Thus, to understand the attracting cycles for the exponential, we need to follow the orbit of 0. Unlike the polynomial case, there is no nice dichotomy based on the fate of the orbit of 0. If the exponential has an attracting cycle, then the basin of attraction of this cycle serves as our analogue for the filled-in Julia sets from

the polynomial cases. Clearly, this basin is open and it is also dense in the plane. We note that the complement of the basin is composed of an uncountable set of curves(hairs), each of which is homeomorphic to a closed half-line.

We now focus on the dynamics of the exponential family , giving a topological analysis via symbolic dynamics.

Let $\mathbb{C}^- = \mathbb{C} - \mathbb{R}^+$, where $\mathbb{R}^+ = \{x \mid x \geq 0\}$. Let $\lambda = re^{i\theta} \in \mathbb{C}^-$. Then, we define horizontal strips $R_\lambda(\ell)$ in \mathbb{C} by

$$R_\lambda(\ell) = \{z \in \mathbb{C} \mid (2\ell - 1)\pi - \theta < \text{Im}z < (2\ell + 1)\pi - \theta\}.$$

Note that the boundaries of the strips are the pre-images of \mathbb{R}^+ under E_λ and that $E_\lambda : R_\lambda(\ell) \rightarrow \mathbb{C}^-$ is an analytic homeomorphism. In particular, $E_\lambda|_{R_\lambda(\ell)}$ covers each $R_\lambda(k)$, for $k \neq \ell$.

Definition 7.2.3. Let $z \in \mathbb{C}$. Define the itinerary of z to be the sequence of integers

$$S(z) = s_0 s_1 s_2 \dots$$

where $s_j = k$ if $E_\lambda^j(z) \in R_\lambda(k)$.

An itinerary, $S(z)$, is *bounded* if $\sup_j |s_j| < \infty$. We restrict our attention to those itineraries which are bounded.

7.2.1 Hairs in the Dynamical Plane

Definition 7.2.4. A tail of a hair with external address $\theta = s_0 s_1 s_2 \dots$ is a continuous curve $h_{\lambda, \theta} : [1, \infty) \rightarrow \mathbb{C}$ satisfying

1. For each $t \geq 1$, the point $h_{\lambda, \theta}(t)$ has itinerary θ .

$$2. \lim_{n \rightarrow \infty} \operatorname{Re}(E_\lambda^{\circ n}(h_{\lambda, \theta}(t))) = +\infty.$$

$$3. \lim_{t \rightarrow +\infty} \operatorname{Re}(h_{\lambda, \theta}(t)) = +\infty.$$

In simple terms, a tail of a hair is a curve of points stretching to infinity, for which all points on the curve share the same itinerary with respect to the partition given in Section 2. By condition 2 of the definition, a tail of a hair lies in the Julia set J_{E_λ} . We use the term *external address* to provide an analogy with external angles for polynomial maps. The following result is proved in [30].

Theorem 7.2.5. *For every $\lambda \in \mathbb{C}^*$ and every bounded sequence $\theta = s_0 s_1 \cdots$, there exists a tail of a hair with external address θ . Furthermore, there is a positive R , depending on λ and θ , such that every $z \in \mathbb{C}$ with itinerary θ , $\operatorname{Re}(E_\lambda^{\circ n}(z)) > R$ for all n , and $\operatorname{Re}(E_\lambda^{\circ n}(z)) \rightarrow +\infty$ as $n \rightarrow +\infty$ lies on that tail of a hair.*

Note that it is possible to parametrize the tail of a hair by

$$h_{\lambda, \theta}(t) = t - \log \lambda + 2\pi i s_0 + O(e^{-t}) \quad (7.1)$$

such that it satisfies the dynamical functional equation

$$h_{\lambda, \sigma(\theta)}(e^t) = E_\lambda(h_{\lambda, \theta}(t)) \quad (7.2)$$

where σ is the one-sided shift. Then, any tail of a hair may be pulled back via 7.2 infinitely often, unless it runs into the singular value. The resulting pull-back is called a *hair*.

The following may be found in [30].

Theorem 7.2.6. *If the singular orbit of E_λ is bounded, then every periodic hair lands at a periodic point.*

7.2.2 Hyperbolic Components in Parameter Plane

The parameter plane for the complex exponential family E_λ is both complicated and beautiful, with a rather strong connection to the polynomials that we have studied in previous sections. See Figure 7.1.

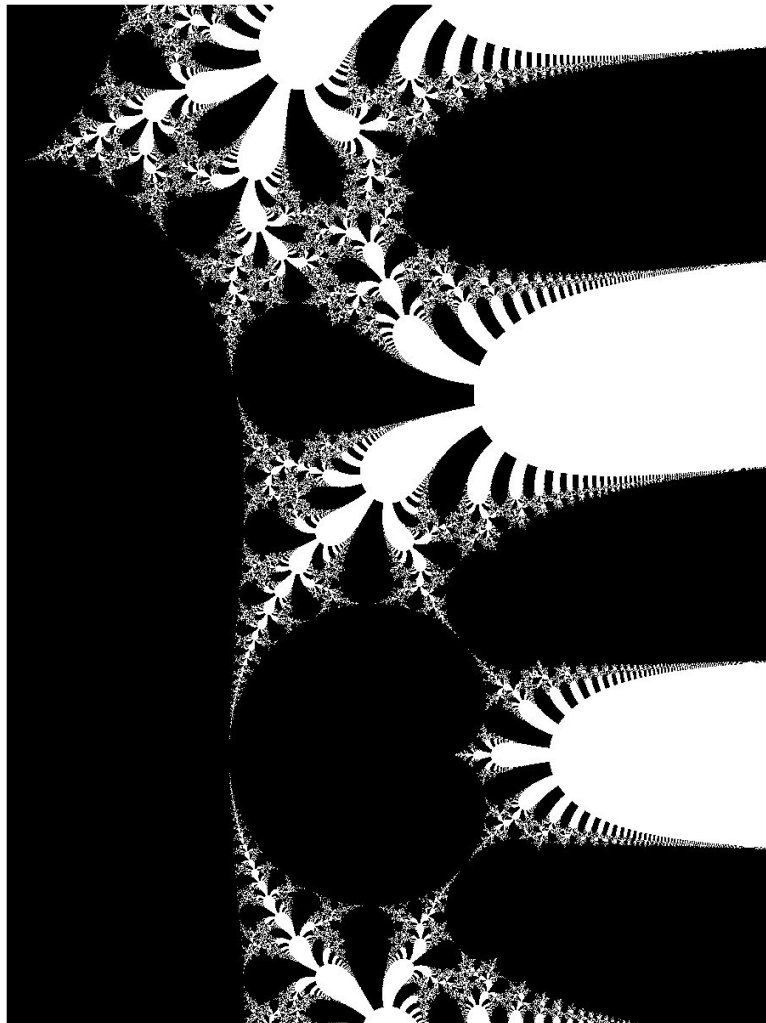


Figure 7.1: The parameter plane for $E_\lambda(z) = \lambda e^z$.

As with the polynomial families that we have studied, the bifurcation diagram,

B_λ , for the exponential family is a picture of the fate of the orbit of 0. The black points in Figure 7.1 correspond to λ values for which the critical orbit is bounded, while white points correspond to λ values for which the critical orbit escapes to infinity. We now begin describe the components of B_λ .

Let $C_N = \{\lambda \in \mathbb{C} : E_\lambda \text{ has an attracting cycle of period } N\}$. Since each C_N is open, $\cup_{N \geq 1} C_N$ is open. A major conjecture is that $B_\lambda = \cup_{N \geq 1} C_N$.

Since the orbit of 0 must be attracted to an attracting or parabolic cycle, it follows that for each λ , E_λ has a unique attracting periodic point, say $z_0 = z_0(\lambda)$. Set $z_j(\lambda) = E_\lambda^j(z_0)$ for $j = 1, \dots, N-1$ and define the multiplier map $\chi : C_N \rightarrow \mathbb{D}$ by $\chi(\lambda) = (E_\lambda^N)'(z_0)$. Since $z_0(\lambda)$ varies analytically with λ , the map χ is analytic.

The region C_1 is special as it is the only bounded set among the C_N . It also has the familiar cardioid shape from the polynomial family. In fact, this is the set of parameters for which E_λ has an attracting fixed point. Note that for $|\mu| < 1$,

$$E_\lambda(z) = \lambda e^z = z \text{ and } E'_\lambda(z) = \lambda e^z = \mu$$

give the following parametrization of C_1 :

$$\lambda = \mu e^{-\mu}.$$

Furthermore, as μ travels around the unit circle, λ wraps once around the boundary of C_1 and at each root of unity, $\lambda \in \partial C_1$ yields E_λ with a fixed point of multiplier an N^{th} root of unity. At these parameter values, there are the bifurcations that we see in B_λ in which one component of C_N meets C_1 . We now describe the components of C_N .

Proposition 7.2.7. *For $N \geq 2$,*

1. *each component of C_N is simply-connected,*
2. *each component of C_N is unbounded, and*
3. *for any connected component W of C_N , the multiplier map $\chi : W \rightarrow \mathbb{D}^*$ is a universal covering map.*

A proof of this proposition may be found in [8].

Now that we have proved the convergence of the spider algorithm for polynomials with an attracting cycle, we extend to exponentials with attracting cycles. Of course, we must make adjustments, but the set-up from the polynomial case was deliberately constructed with the exponential case in mind.

Note that for both of these families of functions, this is a substantial generalization of a case of Thurston's theorem about the topological characterization of rational functions; see [10]. We have removed the restriction that these maps be post-singularly finite. The trade-off is that we now must work with infinite dimensional Teichmüller spaces.

7.3 Exponential Kneading Sequence

Suppose that we want to find a parameter $\lambda \in \mathbb{C}^*$ such that the map $E_\lambda(z) = \lambda e^z$ has an (unique) attracting cycle of length N and with combinatorics specified by a periodic external address, say $\theta = s_0 s_1 \cdots$. In analogy with the polynomial case, we need to find the pre-angles of this θ and assign a dynamically significant kneading

sequence to this address. However, θ is not an angle and so there are no pre-angles, but there is an appropriate analogue.

In the polynomial case, we conjugate to the map $z \mapsto z^d$ and consider the d -tupling map on angles in order to determine pre-angles. This then gives a partition of the plane which leads to itineraries and kneading sequences. In the exponential case, we need the one-sided shift on infinitely many symbols. Note that an external address is an element of the set of infinite sequences

$$\Sigma = \{s_0 s_1 s_2 \cdots : s_j \in \mathbb{Z}\}$$

and the shift map $\sigma : \Sigma \rightarrow \Sigma$ is given by

$$\sigma(s_0 s_1 s_2 \cdots) = s_1 s_2 \cdots.$$

Note that Σ is a topological space with elements ordered lexicographically and σ is a continuous map on this space.

Thus, given an external address $\theta = s_0 s_1 \cdots$, it is easy to see that the preimages of θ under σ are the elements of the set $\{j s_0 s_1 \cdots\}_{j \in \mathbb{Z}}$. We can use these elements to partition Σ . Let (s, r) denote the open interval of elements $t \in \Sigma$ with $r < t < s$ in the lexicographic ordering. Then, the intervals $(j\theta, (j+1)\theta)$ naturally partition the space Σ . We will relate this partition of the symbol space to a partition of dynamical plane given by curves landing at the the singular value.

Let $\theta = s_0 s_1 \cdots$ be a periodic external address. There is exactly one interval $(j\theta, (j+1)\theta)$ of the above partition which contains θ . In fact, one can check that θ lies in one of the two intervals $(s_0\theta, (s_0+1)\theta)$ or $((s_0-1)\theta, s_0\theta)$. Denote this interval by I_0 and label intervals above this interval sequentially with I_1, I_2, \dots and label those below with I_{-1}, I_{-2}, \dots . See Figure 7.2.

Now, let $\tau = t_0 t_1 \cdots$ be any other external address and label its orbit under the shift map by the intervals above. This is called the *itinerary* of τ with respect to the θ partition and it is denoted $\text{Itin}_\theta(\tau)$. It is defined by

$$\text{Itin}_\theta(\tau) = i_0 i_1 i_2 \cdots \quad \text{where } i_k = m \text{ if } \sigma^{\circ k}(\tau) \in I_m.$$

It may occur that iteration of the shift map lands on the boundary of the interval partition. In such a case, we label the itinerary with a boundary symbol. For example, if $\sigma^{\circ k}(\tau)$ lies on the boundary between I_j and I_{j+1} , then we write $i_k = \overset{j+1}{j}$.

Definition 7.3.1. *The kneading sequence of an external address θ is its itinerary with respect to its own partition. That is, $\text{knead}(\theta) = \text{Itin}_\theta(\theta)$.*

For example, we see in Figure 7.2 that the kneading sequence for $\theta = \overline{0102}$ is the repeating sequence 010_1^2 , whereas the itinerary of $\tau = \overline{001}$ with respect to θ is $(-1)00$.

Clearly, the only sequences that contain a boundary symbol are those that eventually map onto θ and if we consider only periodic sequences, then the only ones that contain a boundary symbol are the finitely many shifts of θ . Furthermore, if θ is periodic of period $N > 1$ then the only itinerary that has a boundary symbol in the N^{th} position is θ itself. This leads us to the following lemma on symbolic dynamics.

Lemma 7.3.2. *For any periodic external address $\theta \in \Sigma$ and any periodic itinerary $\alpha \in \Sigma$, there is a periodic external address $\tau \in \Sigma$ such that $\text{Itin}_\theta(\tau) = \alpha$. The number of such sequences τ is always finite.*

Proof. A proof a more general result may be found in [30]. □

Armed with the kneading sequence associated to a periodic external address and Lemma 7.3.2, we can prove the following.

Proposition 7.3.3. *Suppose that E_λ has an attracting periodic cycle of length N . Then, every repelling periodic point is the landing point of at least one and at most, finitely many periodic hairs.*

Proof. The statement that there are at most finitely many landing hairs is the same proof as in the polynomial case and is omitted. See [21], for example. \square

We now suppose that $\lambda \in \mathbb{C}^*$ such that E_λ has an attracting cycle of length, say N . We will define a partition of the dynamical plane in which every repelling periodic point is determined by its itinerary with respect to this partition.

By Proposition 7.3.3, there every repelling periodic point is the landing point of a periodic hair. Further, by a theorem of Schleicher [30], there is a unique repelling periodic point, say ζ , on the boundary of the Fatou component U_1 containing the singular value which is fixed under $E_\lambda^{\circ N}$ and at which at least two periodic hairs land; such a point is called a *characteristic point*. Denote these hairs by h_1 and h_2 with h_1 being the hair with smaller external address, with respect to lexicographic ordering. Next, let Γ be any simple curve within U_1 which connects ζ to the singular value 0 and is invariant under $E_\lambda^{\circ N}$. Such a curve always exists: take infinitely many inverses of E_λ that extend 0. Let $\mathcal{C} = h_1 \cup \Gamma$. Since \mathcal{C} terminates in the singular value 0, the inverse images of \mathcal{C} partition the plane into sectors that are $2\pi i$ translates of each other. There is a unique sector which contains 0; label it by S_0 . Label those sectors above S_0 sequentially with S_1, S_2, \dots and those below S_0 with S_{-1}, S_{-2}, \dots . With this partition, we can prove the following. As usual, we call the *itinerary* of

a point with respect to this partition the sequence of sectors that the orbit of the point visits.

Theorem 7.3.4. *If $E_\lambda(z) = \lambda e^z$ has an attracting cycle, then every repelling periodic point has a well-defined itinerary and no two such points have an identical itinerary. Further, a periodic hair lands at a periodic point if and only if the hair and point have identical itineraries.*

Proof. Let z_1, z_2, \dots and w_1, w_2, \dots be two periodic orbits which share the same itinerary $t_1 t_2 \dots$ with respect to the partition given above. Let m be the least common multiple of the orbit periods of z_1 and w_1 so that $z_1 = z_{m+1}$ and $w_1 = w_{m+1}$; we cannot a priori assume that their orbit periods are equal.

Let $U = \mathbb{C} - \left(\overline{\bigcup_{k>0} E_\lambda^{\circ k}(h_1)} \right)$, where h_1 is the hair described prior to the statement of this theorem. Then, U is an open set and by setting $U_j = U \cap S_j$, we find that each U_j is open and that most U_j are connected. If, however, multiple rays land at ζ , then by Proposition 7.3.3, U_j is composed of finitely many connected components. Each connected component of a given U_j carries its own hyperbolic metric and for every j , there is a branch of E_λ^{-1} mapping U into U_j . Further, the restriction of any such branch to a component of some U_ℓ is a contraction in the hyperbolic metric. We must now consider two cases.

Case 1: There is an index k for which z_k and w_k are in the same connected component of U_{t_k} .

Since z_k and w_k have the same itinerary, there is a common branch of E_λ^{-1} mapping z_k to z_{k-1} and w_k to w_{k-1} and this pull-back shrinks the hyperbolic distance between these points. Repeating this process N times, we return to the points z_k

and w_k , but there hyperbolic distance is reduced. This is a contradiction and hence, $z_1 = w_1$. Now clearly, the period of the itinerary must divide the period of the orbit. If it strictly divides the period of the orbit, then we have two periodic points with the same itinerary which we just showed cannot occur. Hence, the period of the itinerary and the period of the orbit must be the same.

Summing up, any two periodic points must have different periodic itineraries and the period of the orbit of the point equals the period of the itinerary. Since E_λ has an attracting cycle, the orbit of the singular point is bounded and by Proposition 7.3.3, any periodic hair lands at a periodic point. Clearly, the itinerary of the hair and its landing point must be the same. Therefore, any repelling periodic point is the landing point of any ray with the same itinerary. This completes Case 1.

Case 2: The orbits of z_k and w_k are never in the same connected component of U_{t_k} .

If z_k and w_k are in different connected components of U_{t_k} , then they must be separated by hairs landing at some forward image of ζ . Since the itineraries of z_k and w_k are the same, z_{k-1} and w_{k-1} both lie in the same strip $S_{t_{k-1}}$ and the inverse images of the hairs separating z_k and w_k must lie in this sector. Now the number of hairs that separate z_{k-1} and w_{k-1} can only get fewer if their inverse images are in different sectors, but their number never increases. Thus, z_k and w_k can forever be in different connected components of U_{t_k} only if their itinerary is the same as that for the forward image of ζ in U_{t_k} . Denote this forward image of ζ by ζ_k .

Now, connect z_k to a linearizable neighborhood of ζ_k by a curve of finite hyperbolic length. Successive pull-backs will shrink the linearizable neighborhood to ζ_k , while the hyperbolic length of the curve will not have increased. Hence, its

Euclidean length must be zero. Thus, $z_k = \zeta_k$. Similarly, $w_k = \zeta_k = z_k$. Case 2 is proved. \square

7.4 Exponential Spider Space

As we have seen, hairs for exponential maps stretch to $+\infty$ and in a far right plane, they do so with bounded imaginary parts. Thus, it makes sense to model our Standard Exponential Spider by horizontal radial lines from points of the postsingular set along with discs attached. Let $\theta = s_0 s_1 \cdots$ be a periodic external address of period N . List the orbit of θ under the shift operator σ in its proper lexicographic ordering. Thus, we get list of N elements:

$$\sigma^{\circ k_1}(\theta) < \sigma^{\circ k_2}(\theta) < \cdots < \sigma^{\circ k_{N-1}}(\theta).$$

If $\theta = \sigma^0(\theta)$ occurs as the j^{th} entry in this list, renumber the list so that θ is the 0^{th} entry in the list and renumber the entries before θ sequentially with negative numbers and those after θ with positive numbers. Then, for $j = 1, \dots, N$, set x_j equal to the order in which $\sigma^{j-1}(\theta)$ appears in the renumbered list. So, x_1 is always equal to 0. For example, the orbit of $\theta = \overline{0110}$ satisfies

$$\sigma^{\circ 3}(\theta) < \sigma^{\circ 0}(\theta) < \sigma^{\circ 1}(\theta) < \sigma^{\circ 2}(\theta).$$

Instead of calling $\sigma^{\circ 3}(\theta)$ the first element of the ordered set, we call it the -1^{th} element so that θ becomes the 0^{th} element of the list. Then,

$$x_1 = 0, \quad x_2 = 1, \quad x_3 = 2, \quad x_4 = -1.$$

Definition 7.4.1. (Standard Exponential Spider)

The Standard Exponential Spider, $\mathcal{ES}_{\theta, \mu}$, is the set

$$\left(\bigcup_{j=1}^N \overline{D}_j \right) \cup \left(\bigcup_{j=1}^N \gamma_j \right) \cup \{\infty\}$$

where D_j is the disc centered at $-\frac{1}{3} + x_j i$ with radius $\frac{1}{3}$ and $\gamma_j = \{t + x_j i : t \geq 0\}$.

The disc D_j comes with a set of distinguished points which are determined by μ . These points are determined by multiplication of x_j by μ with respect of the center of D_j . This is exactly the same as in the polynomial case. (See Chapter 4.)

As in the polynomial case, our standard exponential spider resembles a fat-footed spider with legs stretching to infinity, with the noticeable difference here that the legs approach infinity along bounded imaginary parts. Since the spiders defined in the polynomial case used little about the fact that we were working with polynomials, much of the work there follows through to the exponential spiders. Hence, we do not re-prove those facts as they appear in the text.

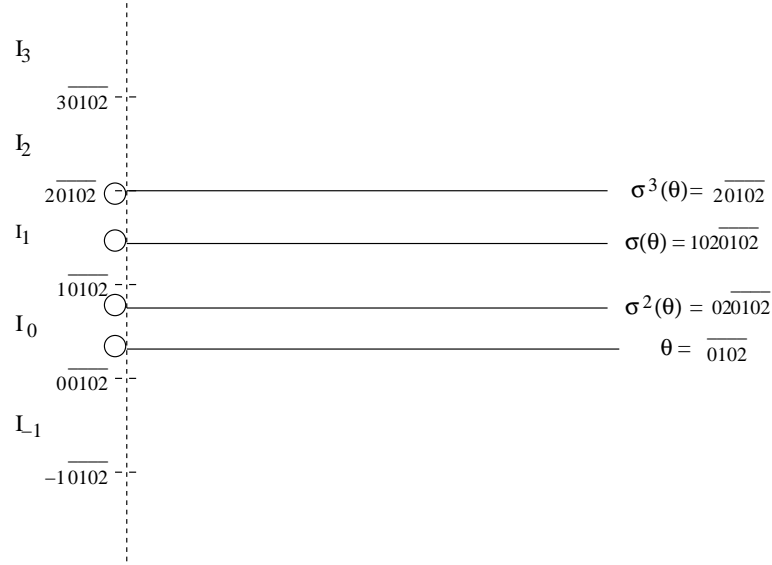


Figure 7.2: Standard Exponential Spider with external address $\overline{0102}$.

Definition 7.4.2. (Exponential Spiders)

An exponential spider is a continuous injective mapping $\varphi : \mathcal{ES}_{\theta, \mu} \rightarrow \hat{\mathbb{C}}$ satisfying:

1. φ is univalent on $\cup D_j$,
2. $\varphi(0) = 0$, $\varphi(\infty) = \infty$, and
3. φ preserves the order of the legs at ∞ .
4. For each $j = 1, \dots, N$, the diameter of $\varphi(D_j)$ is less than 2π .

We denote the set of exponential spiders by $\mathcal{ET}_{\theta, \mu}^0$.

The fourth condition above is necessary since we will apply inverse branches of exponential mappings to these spiders, and we want these branches well-defined. Once again, we refer to $\cup \varphi(D_j)$ as the *feet* of the spider and to $\cup \varphi(\gamma_j)$ as the *legs* of the spider.

Then, the *Exponential Spider Space* is the quotient

$$\mathcal{ET}_{\theta,\mu} = \mathcal{ET}_{\theta,\mu}^0 / \sim,$$

where $\varphi_1 \sim \varphi_2$ if there are scalars $\alpha_j \in \mathbb{C} - \{0\}$ such that $\varphi_1(z) = \alpha_j \varphi_2(z)$ for $z \in \bigcup \overline{D}_j$ and φ_1 is isotopic to φ_2 rel $\varphi_1(\bigcup \overline{D}_j)$.

Theorem 7.4.3. (Properties of $\mathcal{ET}_{\theta,\mu}$)

$\mathcal{ET}_{\theta,\mu}$ is a contractible complex Banach manifold and the tangent space to $\mathcal{ET}_{\theta,\mu}$ at φ is $Z_\varphi \cong Q_\varphi^*$, where Z_φ and Q_φ^* are as in Chapter 5.

Proof. Note that the only difference between the definition of exponential spider space and polynomial spider space is in the direction in which the legs approach infinity. Since this fact was not used in proving this theorem in the polynomial case, the same proof works here. □

7.5 Exponential Spider Mapping

Now, we define the spider mapping $\sigma_\varepsilon : \mathcal{ET}_{\theta,\mu} \rightarrow \mathcal{ET}_{\theta,\mu}$, much the same as in the polynomial case. Set $\lambda = \varphi(x_2)$. Since the leg $\varphi(\gamma_1)$ terminates at 0, the (infinitely many) preimages of this leg under $E_\lambda(z) = \lambda e^z$ stretch from $-\infty$ to $+\infty$ spaced at intervals of $2\pi i$. Thus, these preimages naturally partition the plane into sectors. Note that 0 lies in the interior of one of the sectors by the injectivity of spiders: the only way that 0 could lie on a partition boundary is if λ lies on $\varphi(\gamma_1)$, which injectivity prohibits. Label the sector containing 0 by S_0 , label the sectors above S_0 sequentially by S_1, S_2, \dots , and label those below S_0 sequentially by S_{-1}, S_{-2}, \dots .

Notice that this is much the same partition of the plane that was used in the proof of Theorem 7.3.4.

Let $\text{knead}(\theta) = \alpha_1\alpha_2 \cdots \alpha_N$. For $j = 1, \dots, N - 1$, let $\tilde{\varphi}(x_j)$ be the preimage of $\varphi(x_{j+1})$ that lies in sector S_{α_j} . The leg and foot attached to $\tilde{\varphi}(x_j)$ is the preimage of the $(j + 1)^{\text{th}}$ foot and leg of φ that contains $\tilde{\varphi}(x_j)$. To define the point $\tilde{\varphi}(x_N)$, we note that $\alpha_N = \frac{\ell+1}{\ell}$ for some integer ℓ . As in the polynomial case, we choose the preimage of $\varphi(x_{N+1})$ which lies in sector S_ℓ . We now define the final foot and leg of $\tilde{\varphi}$.

Let \mathcal{A} be the image of the annulus

$$\left\{ z : \frac{|\mu|}{3} < |z - \frac{1}{3}| < 0 \right\} \subset D_1$$

under φ . Then, $\tilde{\varphi}(D_N)$ is the preimage of $D = \varphi(D_1) - \mathcal{A}$ which has $\tilde{\varphi}(x_N)$ on its boundary. Since the distance from 0 to ∂D is bounded away from 0, it follows that $\tilde{\varphi}(\overline{D_N})$ lies in a right half-plane $\{\text{Re}z \geq \nu\}$.

The final leg of $\tilde{\varphi}$ will be composed of the partition curve \mathcal{C} between sectors S_ℓ and $S_{\ell+1}$ and a curve from $-\infty$ to $\tilde{\varphi}(x_N)$. Let Γ be any simple curve connecting 0 to x_{N+1} in $\left\{ z : \frac{|\mu|}{3} < |z - \frac{1}{3}| < 0 \right\} \subset D_1$ with looping defined as in Chapter 4. Then, $E_\lambda^{-1}(\varphi(\Gamma))$ is a curve from $-\infty$ to $\tilde{\varphi}(x_N)$ and the final leg is

$$\tilde{\varphi}(\gamma_N) := \mathcal{C} \cup E_\lambda^{-1}(\varphi(\Gamma)).$$

Since we are only interested in the legs up to homotopy, we may replace $\tilde{\varphi}(\gamma_N)$ with an equivalent leg which only goes as far to the left as $\{\text{Re}z = \nu\}$ and then loops into $\tilde{\varphi}(x_N)$.

Thus, we have specified a new spider $\tilde{\varphi}$ and $\sigma_\mathcal{E} : \mathcal{ET}_{\theta,\mu} \rightarrow \mathcal{ET}_{\theta,\mu}$ is a holomorphic map given by $\sigma_\mathcal{E}([\varphi]) = \tilde{\varphi}$.

7.5.1 Fixed Point of Exponential Spider Mapping

We now show that if the spider mapping has a fixed point, then we have found a parameter λ and a parametrization of the unique attracting cycle with combinatorics defined by the given external address.

Theorem 7.5.1. *Suppose that $[\varphi_\infty]$ is fixed by σ_ε . If $\zeta := \lim_{k \rightarrow \infty} \varphi_\infty(x_{1+kN})$, then*

$$E_\lambda^{\circ N}(\zeta) = \zeta \quad \text{and} \quad (E_\lambda^{\circ N})'(\zeta) = \mu.$$

Moreover, the j^{th} leg of φ_∞ is homotopic to the hair at external address $\sigma^{j-1}(\theta)$, where σ is the shift map on infinitely many symbols.

Proof. Set $\lambda = \varphi_\infty(x_2)$. Since φ_∞ is fixed, we have that $\tilde{\varphi}_\infty(x_j) = \varphi_\infty(x_j)$, for all j . By construction, $E_\lambda(\tilde{\varphi}_\infty(x_j)) = \varphi_\infty(x_{j+1})$. So,

$$\begin{aligned} E_\lambda^{\circ N}(\zeta) &= E_\lambda^{\circ N} \left(\lim_{k \rightarrow \infty} \varphi_\infty(x_{1+kN}) \right) \\ &= E_\lambda^{\circ N} \left(\lim_{k \rightarrow \infty} \tilde{\varphi}_\infty(x_{1+kN}) \right) \\ &= \lim_{k \rightarrow \infty} E_\lambda^{\circ N}(\tilde{\varphi}_\infty(x_{1+kN})) \\ &= \lim_{k \rightarrow \infty} \varphi_\infty(x_{1+(k+1)N}) \\ &= \zeta. \end{aligned}$$

Also note that

$$\varphi_\infty^{-1}|_{\varphi(D(\zeta, |\mu|r))} \circ E_\lambda^{\circ N} \circ \varphi_\infty|_{\varphi^{-1}(D(\zeta, r))} = \mu.$$

□

7.5.2 Convergence to a Fixed Point

We now show that σ_ε converges to a fixed spider $[\varphi_\infty]$ under iteration. As in the polynomial case, we need both a compactness and contraction statement to deduce the existence of a fixed point of the exponential spider mapping. The uniqueness of the fixed point follows from the fact that the Exponential Spider Space is contractible. We begin with the compactness statement.

As in the polynomial case, when an exponential mapping has an attracting periodic point of period N , there is a constant $C = C(\mu)$ such that

$$|E_\lambda^{\circ n}(0)| > C, \quad \text{for all } n.$$

This is easy to see by looking at the attracting cycle under linearizing coordinates.

Lemma 7.5.2. *Let C be as above and let $0 < \epsilon < C/2$. Define $\mathcal{ET}_{\theta,\mu}^\epsilon \subset \mathcal{ET}_{\theta,\mu}$ to be the set of spiders for which the discs centered at $\varphi(x_j)$ with radii ϵ^j are all disjoint for $j \geq 1$. Then, $\mathcal{ET}_{\theta,\mu}^\epsilon$ is invariant under the spider mapping.*

Proof. Set $\lambda = \varphi(x_2)$. Note that $\varphi(x_1) = 0$ and that

$$E_\lambda^{-1}(D(0, \epsilon)) = \left\{ z : \operatorname{Re} z \leq \log \left(\frac{\epsilon}{|\lambda|} \right) \right\}.$$

That is, the preimage of a disc about zero contains some left half-plane. Since $D(0, \epsilon)$ does not contain any of the points $\varphi(x_j)$, for $j \geq 2$, it follows that $E_\lambda^{-1}(D(0, \epsilon))$ does not contain any of the points $\tilde{\varphi}(x_j)$ for $j \geq 1$. So, if $\operatorname{Re}(w) > \log \left(\frac{\epsilon}{|\lambda|} \right)$, then

$$|E'_\lambda(w)| = |\lambda e^w| = |\lambda| e^{\operatorname{Re} w} > |\lambda| \frac{\epsilon}{|\lambda|} = \epsilon.$$

Hence, for $\operatorname{Re}(E_\lambda^{-1}(z)) > \log \left(\frac{\epsilon}{|\lambda|} \right)$, we have

$$\left| (E_\lambda^{-1})'(z) \right| = \frac{1}{|E'_\lambda(E_\lambda^{-1}(z))|} < \frac{1}{\epsilon}.$$

Now, if z lies within the disc of radius e^{j+1} about $\varphi(x_{j+1})$, then $\tilde{z} = E_\lambda^{-1}(z)$ lies in a disc about $\tilde{\varphi}(x_j)$ of radius $\frac{1}{\epsilon}e^{j+1} = \epsilon^j$. If there is were a point in the intersection of the discs in the preimage, then the image of such a point would lie in the intersection of the image discs, which is a contradiction. \square

Now, we discuss the contraction, showing that E_λ is contracting for an infinitesimal metric on the tangent space to spider space. More precisely, as in the polynomial case, we have that the derivative $(d_\varphi\sigma_\epsilon)^*$ is dual to the push-forward operator $(E_\lambda)_*$ on $Q_{\tilde{\varphi}}$. The push-forward is defined by

$$(E_\lambda)_*q := \sum_L L^*q,$$

where the sum is taken over all branches, L , of E_λ^{-1} .

Lemma 7.5.3.

$$\|(E_\lambda)_*\| = \left\{ \sup_{q \in Q_{\tilde{\varphi}} - 0} \frac{\|(E_\lambda)_*q\|}{\|q\|} \right\} < 1.$$

Proof. By the triangle inequality, we easily see that

$$\|(E_\lambda)_*q\| \leq 1$$

and by virtue of all the preimages that we discard in defining the spider mapping, we have the statement of the lemma. \square

Combining these lemmas yields

Theorem 7.5.4. *The spider mapping σ_ϵ has a unique fixed point, $[\varphi_\infty]$.*

Theorem 7.5.5. *For any $N \geq 3$ and any bounded periodic sequence $\theta = s_0s_1 \dots$, there is a hyperbolic component W in the parameter space for $E_\lambda(z) = \lambda e^z$ such that*

for each $\lambda \in W$, the hair $h_{\lambda, \theta}$ lands at the characteristic repelling periodic point on the boundary of the Fatou component containing 0. Any such hyperbolic component is uniquely specified by the sequence θ .

Proof. Clearly, by Theorem 7.5.1, the existence of a fixed point of the spider mapping proves the first part of the corollary. Uniqueness follows from the uniqueness of external addresses, as W can be encoded by the hair of address θ . \square

Bibliography

- [1] L. Ahlfors, “Lectures on Quasiconformal Mappings”, Van Nostrand, 1966.
- [2] P. Blanchard, *Complex analytic dynamics on the Riemann sphere*, Bull. AMS **11**, 1984.
- [3] B. Bielefeld, Y. Fisher, and J. Hubbard, *The classification of critically preperiodic polynomials as dynamical systems*, Jour. AMS **5** (1992) 721-762.
- [4] B. Branner and J. Hubbard, *The iteration of cubic polynomials*, part I: *The global topology of parameter space*, Acta Math. **160**, 1988.
- [5] L. Carleson and T. Gamelin, “Complex Dynamics”, Springer-Verlag, 1993.
- [6] G. Cui, Y. Jiang, and D. Sullivan, *Combinatorics of geometrically finite rational maps*, preprint, 1998.
- [7] R. Devaney, “An Introduction to Chaotic Dynamical Systems”, Perseus Publishing, 1989. .
- [8] R. Devaney, L. Goldberg, and J. Hubbard, *Dynamical approximation to the exponential map via polynomials*, MSRI preprint, 1986.
- [9] A. Douady and J. Hubbard, *Etude dynamique des polynômes complexes*, Publications Math. d’Orsay **84-02** (1984) (première partie) and **85-04** (1985) (deuxième partie).
- [10] A. Douady and J.H. Hubbard, *A proof of Thurston’s topological characterization of rational functions*, Acta Math. **171** (1993), 263-297.
- [11] R. Devaney, X. Jarque, and N. Fagella, *Hyperbolic components of the Complex Exponential Family*, manuscript, 2001.

- [12] D. Eberlein, *Rational Parameter Rays of Multibrot Sets*, Diploma Thesis, Technische Universität München, 1999.
- [13] F. Gardiner and N. Lakic, “Quasiconformal Teichmüller Theory”, AMS Mathematical surveys and monographs, Vol. **76** 2000.
- [14] J.H. Hubbard, “Teichmüller Theory and Three Theorems of Thurston,” manuscript, in preparation.
- [15] J.H. Hubbard and D. Schleicher, *The Spider Algorithm*, In: *Complex dynamics: the mathematics behind the Mandelbrot and Julia sets*, AMS Proceedings of the Symposia in Applied Mathematics, Vol. **49**, 1994.
- [16] B. Krauskopf and H. Kriete, *Kernel convergence of hyperbolic components*, Ergodic Theory and Dyn. Sys. **17** (1997), 1137-1146.
- [17] O. Lehto, “Univalent Functions and Teichmüller Spaces”, Springer-Verlag, Graduate Texts in Mathematics **109**, 1987.
- [18] G. S. Lieb, *Holomorphic Motions and Teichmüller Space*, Ph.D. Dissertation, Cornell University, New York, 1990.
- [19] N. Lakic, *Infinitesimal Teichmüller geometry*, Complex Variables **30**, 1996.
- [20] T. Lei, editor, “The Mandelbrot Set, theme and variations”, London Math Soc. Lecture Notes **274**, Cambridge University Press, 2000.
- [21] J. Milnor, “Dynamics in one complex variable: introductory lectures”, Friedr. Vieweg & Sohn, Braunschweig, 1999.
- [22] J. Milnor, *Periodic orbits, external rays, and the Mandelbrot set: an expository account*, Astérisque **261**, 2000.
- [23] J. Milnor, *Hyperbolic components in spaces of polynomial maps*, Stony Brook Preprint 1992, #3.
- [24] C. McMullen, “Complex Dynamics and Renormalization,” Ann. Math. Studies **135**, Princeton Univ. Press (1994).
- [25] C. McMullen, *Iteration on Teichmüller Space*, Invent. Math. **9**, 1990.
- [26] S. Mitra, “Teichmüller theory and holomorphic motions”, Ph.D. thesis, Cornell University, 1999.

- [27] C. McMullen and D. Sullivan, *Quasiconformal homeomorphisms and dynamics III: The Teichmüller space of a holomorphic dynamical system*, Advances in Mathematics **135**, 1998.
- [28] A. Poirier, *On postcritically finite polynomials, parts 1 and 2*, Stony Brook IMS preprints **5** and **7**, 1993.
- [29] D. Schleicher, “Internal addresses and in the Mandelbrot set and irreducibility of polynomials,” Ph.D. Thesis, Cornell University, 1994.
- [30] D. Schleicher and J. Zimmer, “Dynamic rays for exponential maps,” Stony Brook IMS preprint **9**, 1999.
- [31] D. Schleicher, “Attracting dynamics of exponential maps,” Manuscript, 2000.
- [32] N. Steinmetz, “Rational Iteration”, De Gruyter Studies in Mathematics **16**, 1993.